

Consensus-Based Odor Source Localization by Multiagent Systems

Abhinav Sinha^{ID}, Ritesh Kumar, Rishemjit Kaur, and Amol P. Bhondekar

Abstract—This paper presents an investigation of the task of localizing unknown source of an odor by heterogeneous multiagent systems. A hierarchical cooperative control strategy has been proposed as a potential candidate to solve the problem. The agents are driven into consensus as soon as the information about the location of source is acquired. The controller has been designed in a hierarchical manner of group decision making, agent path planning, and robust control. In group decision making, particle swarm optimization algorithm has been used along with the information of the movement of odor molecules to predict the odor source location. Next, a trajectory has been mapped using this predicted location of source, and the information is passed to the control layer. A variable structure control has been used in the control layer due to its inherent robustness and disturbance rejection capabilities. Cases of movement of agents toward the source under consensus, and parallel formation have been discussed. The efficacy of the proposed scheme has been confirmed by simulations.

Index Terms—Decentralized cooperative control, heterogeneous multiagent systems (MASs), inverse sine hyperbolic reaching law, odor source localization (OSL), robot olfaction, sliding mode control (SMC).

I. INTRODUCTION

RESEARCH in robot olfaction has received wide attention to address many challenges, some of which include detection of hazardous gases in mines, tunnels and industrial setup, search and rescue of victims, forest fire detection and firefighting [1]–[3], etc. Recently, extra-terrestrial odor source localization via autonomous agents has been carried out on Mars [4], [5]. Numerous simple and complex algorithms for olfaction problems have imitated behavior of biological entities, such as mate seeking by moths, foraging by lobsters, prey tracking by mosquitoes and blue crabs, etc. However, techniques like probabilistic inference [6], [7]; robust control [8]; swarm intelligence [9]; biased random walk [10]; and

optimization and meta-heuristics prove better in localization than aforementioned techniques.

Works on OSL in early 90s were mostly targeted via chemical gradient-based techniques in a diffusion dominated environment [11]–[14]. Attributed to geometry and dimensions of the above-ground agents, this assumption leads to suboptimal performance. This assumption, however, yields satisfactory performance in underground search [15]–[17]. Difficulties associated with diffusion dominated odor dispersal model led to the development of reactive plume tracking approaches, the performance of which was further improved by combining vision with sensing [18]–[20]. The efficiency of techniques depending heavily on sensing, such as chemotaxis [21]; anemotaxis [6], [22]; infotaxis [7]; fluxotaxis [23] and their close variants are limited by the quality of sensors and the manner in which they are used. Bio-inspired agent maneuvering such as Braitenberg style [24], *E. coli* algorithm [10], zigzag dung beetle approach [25], and silkworm moth style [15], [26], [27] are slow in localization. Many of these localizing techniques deliver unsatisfactory tracking performance in a turbulence dominated environment.

With advantages of multiagent systems such as spatial diversity, distributed sensing and actuation, redundancy, scalability, high reliability, and increased probability of success, OSL can be effectively solved. This dynamical optimization problem is characterized by three stages: 1) instantaneous plume sensing (plume finding); 2) maneuvering of the agents (plume traversal); and 3) cooperative control of the agents. In spite of growing attention from researchers in the last decade [28]–[31], only a few works have addressed OSL using MAS. A distributed cooperative algorithm based on swarm intelligence was put forth by Hayes *et al.* [32] and experimental results proved multiple robots perform more efficiently than a single autonomous robot. Marques *et al.* [33] proposed particle swarm optimization (PSO) algorithm [34] to localize odor source. Studies in [35] reported modified PSO technique based on electrical charge theory by using neutral and charged robots to find the odor source without getting trapped into a local maximum concentration. Cooperative control based on simplified PSO was proposed by Lu *et al.* [36], which is a type of proportional-only controller and the operating region is confined between the global and the local best. This requires complicated obstacle avoidance algorithms and more energy consumption. Odor propagation is nontrivial, i.e., odor arrives in packets, leading to wide fluctuations in measured concentrations. Plumes also tend to be dynamic and turbulent. In order to effectively solve OSL problem, information of wind needs

Manuscript received January 18, 2018; revised May 6, 2018; accepted September 2, 2018. This paper was recommended by Associate Editor L. Zhang. (*Corresponding author: Abhinav Sinha*.)

A. Sinha is with the Indian Institute of Technology Bombay, Mumbai, India (e-mail: sinha.abhinav@iitb.ac.in).

R. Kumar, R. Kaur, and A. P. Bhondekar are with CSIR-Central Scientific Instruments Organisation, Chandigarh, India (e-mail: riteshkr@csio.res.in; rishemjit.kaur@csio.res.in; amolbhondekar@csio.res.in).

This paper has supplementary downloadable material available at <http://ieeexplore.ieee.org>, provided by the author.

Color versions of one or more of the figures in this paper are available online at <http://ieeexplore.ieee.org>.

Digital Object Identifier 10.1109/TCYB.2018.2869224

83 to be taken into consideration. As odor molecules travel down-
 84 wind, direction of wind provides an effective information on
 85 relative position of the source. Using both concentration and
 86 wind information, Lu and Han have designed a particle filter-
 87 based cooperative control scheme [37] to coordinate multiple
 88 robots toward odor source. However, the dynamical model
 89 used in [36] and [37] are oversimplified to integrator dynamics
 90 and the effects of unknown perturbations have not been con-
 91 sidered. To address the effect of perturbations, robust control
 92 protocols have been designed in [8] and [38], but dynamics of
 93 the agents is homogeneous, i.e., agents are identical. In prac-
 94 tice, it is very difficult to obtain truly homogeneous agents.
 95 Even truly homogeneous agents exhibit a tendency to drift
 96 toward heterogeneity over time and continued operation.

97 In spite of rapid developments in sensor technology, avail-
 98 ability of faster localization algorithms are still a challenge.
 99 Motivated by these studies and in order to effectively address
 100 the OSL problem, we have proposed a three-layered hierar-
 101 chical cooperative control scheme which uses concentraion
 102 information from swarm, as well as wind information from a
 103 measurement model [39] describing movement of filaments to
 104 locate the odor source. Information about the source via instan-
 105 taneous sensing and swarm intelligence is obtained in the first
 106 layer. Second layer is designed to maneuver the agents via tra-
 107 ditional surging, casting, and searching methods. Third layer is
 108 the cooperative control layer and the controller is based on the
 109 paradigms of variable structure control [also known as sliding
 110 mode control (SMC)], which is known for its inherent robust-
 111 ness and properties to reject disturbances that lie in the range
 112 space of input. In the third layer, the information obtained in
 113 the first layer is passed as a reference to the tracking controller.
 114 A block diagram representation of the proposed scheme has
 115 been shown in Fig. 1.

116 The idea of using a finite time controller is not new, how-
 117 ever, we have adopted a different perspective in this paper.
 118 To the best of authors' knowledge, SMC technique has been
 119 used for the first time in OSL. Novel sliding manifold and
 120 reaching law provide faster convergence. The sole idea to
 121 use such a control is to guarantee faster convergence, com-
 122 plete disturbance rejection, and steady precision. Moreover,
 123 studies in this paper incorporate a large class of systems
 124 that may contain unknown inherent nonlinearity and hetero-
 125 geneity. We summarize our contributions via the following
 126 points.

- 127 1) Individual autonomous agents may have some inherent
 128 nonlinear dynamics. This paper generalizes the problem
 129 by taking into account nonlinear dynamics of MAS.
 130 When the uncertain function is zero, the dynamics
 131 simply reduces to that of an integrator system.
- 132 2) Individual autonomous agents might have different
 133 dynamics for a practical application. Hence, the con-
 134 sideration of heterogeneous agent dynamics is closer to
 135 real situations.
- 136 3) The finite time robust controller is based on sliding
 137 modes with nonlinear sliding hyperplane and novel
 138 inverse sine hyperbolic reaching law. Consequently, the
 139 control signal is smooth and reachability to the manifold
 140 is fast.

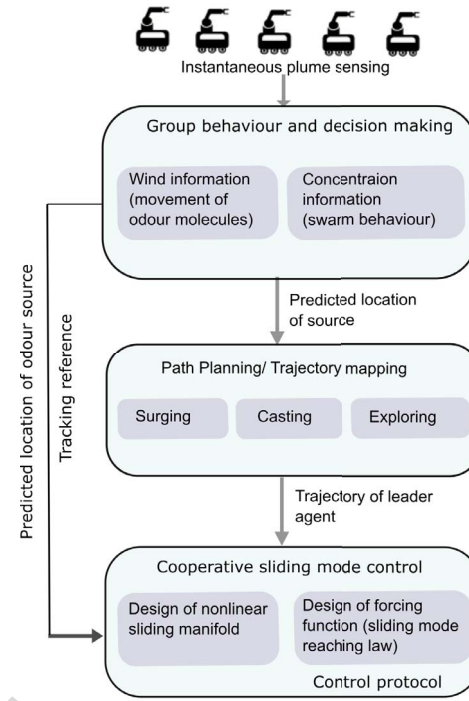


Fig. 1. Proposed hierarchical cooperative control scheme for odor source localization.

4) The synthesized control ensures stability even in the presence of disturbances that are bounded and matched. After introduction to the study in Section I, remainder of this paper is organized as follows. Section II provides insights into preliminaries of spectral graph theory and SMC. Section III presents dynamics of MAS and mathematical problem formulation, followed by hierarchical decentralized cooperative control scheme in Section IV. Results and discussions have been carried out in Section V, followed by concluding remarks in Section VI. We have provided a supplement to this paper with some additional illustrations to aid the propositions.

II. PRELIMINARIES

A. Spectral Graph Theory for Multiagent Systems

A directed graph, also known as digraph is represented throughout in this paper by $\mathcal{G} = (\mathcal{V}, \mathcal{E}, \mathcal{A})$. \mathcal{V} is the nonempty set in which finite number of vertices or nodes are contained such that $\mathcal{V} = \{1, 2, \dots, N\}$. \mathcal{E} denotes directed edge and is represented as $\mathcal{E} = \{(i, j) \forall i, j \in \mathcal{V} \& i \neq j\}$. \mathcal{A} is the weighted adjacency matrix such that $\mathcal{A} = a(i, j) \in \mathbb{R}^{N \times N}$. The possibility of existence of an edge (i, j) occurs if and only if the vertex i receives the information supplied by the vertex j , i.e., $(i, j) \in \mathcal{E}$. Hence, i and j are termed neighbors. The set \mathcal{N}_i contains labels of vertices that are neighbors of the vertex i . For the adjacency matrix \mathcal{A} , $a(i, j) \in \mathbb{R}_0^+$. If $(i, j) \in \mathcal{E} \Rightarrow a(i, j) > 0$. If $(i, j) \notin \mathcal{E}$ or $i = j \Rightarrow a(i, j) = 0$. The Laplacian matrix \mathcal{L} [40] is central to the consensus problem and is given by $\mathcal{L} = \mathcal{D} - \mathcal{A}$ where degree matrix, \mathcal{D} is a diagonal matrix, i.e., $\mathcal{D} = \text{diag}(d_1, d_2, \dots, d_n)$ whose entries are $d_i = \sum_{j=1}^n a(i, j)$. A directed path from vertex j to vertex i defines a sequence comprising of edges $(i_1, i_1), (i_1, i_2), \dots, (i_l, j)$ with distinct vertices $i_k \in \mathcal{V}, k = 1, 2, 3, \dots, l$. Incidence matrix \mathcal{B} is also a

diagonal matrix with entries 1 or 0. The entry is 1 if there exists an edge between leader agent and any other agent, otherwise it is 0. Furthermore, it can be inferred that the path between two distinct vertices is not uniquely determined. However, if a distinct node in \mathcal{V} contains directed path to every other distinct node in \mathcal{V} , then the directed graph \mathcal{G} is said to have a spanning tree. Consequently, the matrix $\mathcal{L} + \mathcal{B}$ has full rank [40]. Physically, each agent has been modeled by a vertex or node and the line of communication between any two agents has been modeled as a directed edge.

182 B. Sliding Mode Control

SMC [41] is known for its inherent robustness. The switching nature of the control is used to nullify bounded disturbances and matched uncertainties. Switching happens about a hypergeometric manifold in state space known as sliding manifold, surface, or hyperplane. The control drives the system monotonically toward the sliding surface, i.e., trajectories emanate and move toward the hyperplane (reaching phase). System trajectories, after reaching the hyperplane, get constrained there for all future time (sliding phase), thereby ensuring the system dynamics remains independent of bounded disturbances and matched uncertainties.

In order to push state trajectories onto the surface $s(x)$, a proper discontinuous control effort $u_{\text{SM}}(t, x)$ needs to be synthesized satisfying the inequality

$$197 \quad s^T(x)\dot{s}(x) \leq -\eta \|s(x)\| \quad (1)$$

with η being positive and is referred as the reachability constant

$$200 \quad \therefore \dot{s}(x) = \frac{\partial s}{\partial x}\dot{x} = \frac{\partial s}{\partial x}f(t, x, u_{\text{SM}}) \quad (2)$$

$$201 \quad \therefore s^T(x)\frac{\partial s}{\partial x}f(t, x, u_{\text{SM}}) \leq -\eta \|s(x)\|. \quad (3)$$

The motion of state trajectories confined on the manifold is known as *sliding*. Sliding mode exists if the state velocity vectors are directed toward the manifold in its neighborhood. Under such consideration, the manifold is called attractive, i.e., trajectories starting on it remain there for all future time and trajectories starting outside it tend to it in an asymptotic manner. Hence, in sliding motion

$$209 \quad \dot{s}(x) = \frac{\partial s}{\partial x}f(t, x, u_{\text{SM}}) = 0. \quad (4)$$

$u_{\text{SM}} = u_{\text{eq}}$ is a solution, generally referred as equivalent control, is not the actual control applied to the system but can be thought of as a control that must be applied on an average to maintain sliding motion, and is mainly used for analysis of sliding motion.

215 III. DYNAMICS OF MAS AND PROBLEM FORMULATION

216 Consider first-order heterogeneous MAS with a virtual leader and a finite number of followers interacting among 218 themselves and their environment in a well-defined directed 219 topology. Via interagent communication, only local information about the predicted location of source of the odor

through instantaneous plume sensing is available. The governing dynamics of first-order heterogeneous MAS that comprise of N agents can be written mathematically as

$$221 \quad \dot{x}_i(t) = f_i(x_i(t)) + u_{\text{SM}_i}(t) + \xi_i; i \in [1, N] \in \mathbb{N} \quad (5) \quad 224$$

where $f_i(\cdot)$ denotes the uncertain dynamics of each agent. x_i and u_{SM_i} are the state of i th agent and the associated control, respectively. ξ_i represents bounded exogenous disturbances that enter the system from input channel, i.e., $\|\xi_i\| \leq \xi_{\max} < \infty$. There is always a limit on how fast a function can change. Considering the functions describing the dynamics (5) do not become infinitely steep at some point, it is safe to assume that the functions satisfy Lipschitz continuity.

Assumption 1: $f_i(\cdot) : \mathbb{R}^+ \times X \rightarrow \mathbb{R}^m$ is locally Lipschitz over some domain $\mathbb{D}_{\mathbb{L}}$ with Lipschitz constant \bar{L} . For our case, we shall take this domain $\mathbb{D}_{\mathbb{L}}$ to be fairly large. $X \subset \mathbb{R}^m$ is a domain in which origin is contained.

Since the function $f_i(\cdot)$ is uncertain, a nominal system model can be extracted from the known part of the uncertain function $f_i(\cdot)$, and the unknown part can be treated by worst case bounds. The dynamics of each agent is affected by the interconnection among agents as well as the presence of inherent nonlinearity in each agent. Note that when $f_i(\cdot) = 0$, the dynamics reduce to those of integrator systems. Similarly, when $f_i(\cdot)$ are all same, we obtain a set of homogeneous agents.

Remark 1: For the sake of simplicity, we shall carry out the discussion in \mathbb{R}^1 . However, the same can be extended to higher dimensions by the use of Kronecker products.

Odor molecules tend to disperse heavily in the environment characterized by diffusion. In making assumptions of a diffusion dominated environment, several factors are ignored. A more realistic picture must include effects of wind, turbulence diffusion, and thermal effects. However, effects of turbulence are difficult to be described mathematically. In addition to the effects of wind, the characteristics of environment can also be described by advection phenomenon. Hence, we have considered a diffusion–advection plume model in our discussed source localization problem. Before we begin to use this model, the following assumptions need to be stated.

Assumption 2: We assume near uniform airflow velocity for all time and throughout the domain in which the task of source localization is being performed.

If the domain is characterized by nonuniform airflow velocity, the concentration of odor molecules in a particular region shall vary too rapidly with time and could possibly result in loss of effective sensing, disordering of swarm, and delayed consensus.

Assumption 3: The turbulence diffusion coefficient K needs to be known beforehand via some suitable measurements. In case K is not known beforehand, then K should be estimated or correlated as a function of wind velocity, i.e., $K = f(v_a)$. This estimation can be performed during the experiment with the data obtained through sensors (e.g., anemometers and gas sensors).

Knowledge of these parameters is essential in algorithm research. These parameters influence the overall effective sensing and accuracy of the prediction of odor source location (the global concentration maxima.) The diffusion–advection model

278 provided in [42] and [43] has been recalled here to simulate
 279 the dynamic plume under time varying disturbances. A steady
 280 concentration profile for a very large span of time ($t \rightarrow \infty$)
 281 can be written as

$$282 \quad C(\vec{r}, \infty) = \frac{q_0}{2\pi K d_i} \exp\left\{-\frac{v_a}{2K}(d_i - \vec{r} + \vec{r}_0)\right\}. \quad (6)$$

283 In (6), $\vec{r}_0 = x_s(t)$ represents the coordinates of the odor
 284 source, $d_i = \|x_i - x_s\|$, q_0 is the filament release rate and
 285 K is the turbulent diffusion coefficient that is independent of
 286 the diffusing material.

287 The problem of odor source localization can be viewed as a
 288 cooperative control problem in which control laws u_{SM_i} need
 289 to be designed such that the conditions $\lim_{t \rightarrow \infty} \|x_i - x_j\| = 0$
 290 and $\lim_{t \rightarrow \infty} \|x_i - x_s\| \leq \theta$ are satisfied. Here, x_s represents
 291 the probable location of odor source and θ is an accuracy
 292 adjustment parameter in declaration of the true location of the
 293 source.

294 IV. HIERARCHICAL DECENTRALIZED COOPERATIVE 295 CONTROL SCHEME

296 In order to force the agents in consensus to locate the source
 297 of odor, we have come up with the following hierarchical
 298 scheme.

299 A. Group Decision Making

300 This layer utilizes both concentration and wind information
 301 to predict the location of odor source. Thus, the final probable
 302 position of the source can be described as

$$303 \quad \phi(t_h) = k_1 p_i(t_h) + (1 - k_1) q_i(t_h). \quad (7)$$

304 With the knowledge of PSO, $p_i(t_h)$ in (7) can be described as
 305 the oscillation center. Information of the wind is captured in
 306 $q_i(t_h)$. $k_1 \in (0, 1)$ denotes additional weighting coefficient.

307 *Remark 2:* Since the sensors equipped with the agents can
 308 only receive data at discrete instants, the arguments in (7)
 309 represent data captured at $t = t_h$ instants ($h = 1, 2, \dots$).

310 It should be noted that ϕ is the tracking reference that is fed
 311 to the tracking controller. Now, we present detailed description
 312 of obtaining $p_i(t_h)$ and $q_i(t_h)$.

313 Commonly used simple PSO algorithm can be described in
 314 the following form:

$$315 \quad v_i(t_{h+1}) = \omega v_i(t_h) + u_{PSO}(t_h) \quad (8)$$

$$316 \quad x_i(t_{h+1}) = x_i(t_h) + v_i(t_{h+1}). \quad (9)$$

317 Here, ω is the inertia factor, $v_i(t_h)$ and $x_i(t_h)$ represent the
 318 respective velocity and position of i th agent. This commonly
 319 used form of PSO can also be used as a proportional-only type
 320 controller, however, for the disadvantages highlighted earlier,
 321 we do not regard PSO as our final controller. PSO control law,
 322 u_{PSO} can be described as

$$323 \quad u_{PSO} = \alpha_1(x_l(t_h) - x_i(t_h)) + \alpha_2(x_g(t_h) - x_i(t_h)). \quad (10)$$

324 In (10), $x_l(t_h)$ denotes the previous best position and $x_g(t_h)$
 325 denotes the global best position of neighbors of i th agent
 326 at time $t = t_h$, and α_1 and α_2 are acceleration coefficients.
 327 Since, every agent in MAS can get some information about the

magnitude of concentration via local communication, position
 328 of the agent with the global best can be easily known. By the
 329 idea of PSO, we can compute the oscillation center $p_i(t_h)$ as
 330

$$331 \quad p_i(t_h) = \frac{\alpha_1 x_l(t_h) + \alpha_2 x_g(t_h)}{\alpha_1 + \alpha_2} \quad (11)$$

332 where

$$333 \quad x_l(t_h) = \arg \max_{0 < t < t_{h-1}} \{g(x_l(t_{h-1})), g(x_i(t_h))\} \quad (12)$$

$$334 \quad x_g(t_h) = \arg \max_{0 < t < t_{h-1}} \left\{ g(x_g(t_{h-1})), \max_{j \in N} a_{ij} g(x_j(t_h)) \right\}. \quad (13)$$

335 Thus, from (10) and (11)

$$336 \quad u_{PSO}(t_h) = (\alpha_1 + \alpha_2)\{p_i(t_h) - x_i(t_h)\} \quad (14)$$

337 which is clearly a proportional-only controller with propor-
 338 tional gain $\alpha_1 + \alpha_2$, as highlighted earlier.

339 In order to compute $q_i(t_h)$, movement process of a single fil-
 340 ament that consists several odor molecules has been modeled
 341 based on the study in [39]. If $x_f(t)$ denotes position of the fil-
 342 ament at time t , $\bar{v}_a(t)$ represent mean airflow velocity and $n(t)$
 343 be some random process, then the model can be described as

$$344 \quad \dot{x}_f(t) = \bar{v}_a(t) + n(t). \quad (15)$$

345 Without loss of generality, we shall regard the start time of
 346 our experiment as $t = 0$. From (15), we have

$$347 \quad x_f(t) = \int_0^t \bar{v}_a(\tau) d\tau + \int_0^t n(\tau) d\tau + x_s(0). \quad (16)$$

348 $x_s(0)$ denotes the real position of the odor source at $t = 0$.

349 *Assumption 4:* We assume the presence of a single, station-
 350 ary odor source. Thus, $x_s(t) = x_s(0)$.

351 Presence of a single source implies that there is only one
 352 global concentration in the domain. Due to nontrivial nature
 353 of odor propagation, discrete packets (or puffs) containing
 354 odor molecules are obtained. Since, concentration of each puff
 355 can be measured, the global maximum concentration can be
 356 established. Implications from Remark 2 require (16) to be
 357 implemented at $t = t_h$ instants. Hence,

$$358 \quad x_f(t_h) = \sum_{m=0}^t \bar{v}_a(\tau_m) \Delta t + \sum_{m=0}^t n(\tau_m) \Delta t + x_s(t_h) \quad (17)$$

$$359 \quad x_f(t_h) = x_s(t_h) + \bar{v}_a^*(t_h) + w^*(t_h). \quad (18)$$

360 In (18), $\sum_{m=0}^t \bar{v}_a(\tau_m) \Delta t = \bar{v}_a^*(t_h)$ and $\sum_{m=0}^t n(\tau_m)$
 361 $\Delta t = w^*(t_h)$.

362 *Remark 3:* In (18), the accumulated average of $\bar{v}_a^*(t_h)$ and
 363 $w^*(t_h)$ can also be considered for all possible filament releas-
 364 ing time.

365 From (18)

$$366 \quad x_f(t_h) - \bar{v}_a^*(t_h) = x_s(t_h) + w^*(t_h). \quad (19)$$

367 The above relationship, (19) can be viewed as the information
 368 about $x_s(t_h)$ with some noise $w^*(t_h)$. Hence,

$$369 \quad q_i(t_h) = x_s(t_h) + w^*(t_h). \quad (20)$$

370 Therefore, ϕ in (7) can now be constructed from (11) and (20).
 371 To summarize, concentration information is obtained via
 372 swarm algorithm, and the wind information is obtained using
 373 a measurement model that describes the movement of odor

374 molecules. Combining this two information together gives the
 375 probable location of the odor source, which is fed to the
 376 tracking controller.

377 B. Path Planning

378 The detection of information of interest based on instant-
 379 aneous sensing of plume depends on the threshold value
 380 of sensors, and the next state is decided according to this
 381 threshold. Hence, the blueprints of trajectory planning can be
 382 described in terms of the following behavior.

- 383 1) *Surging*: If the i th agent receives data well above thresh-
 384 old, we say that some clues about the location of the
 385 source have been detected. If the predicted position of
 386 the source at $t = t_h$ as seen by i th agent be given
 387 as $x_{s_i}(t_h)$, then the next state of the agent is given
 388 mathematically as

$$389 \quad x_i(t_{h+1}) = x_{s_i}(t_h). \quad (21)$$

- 390 2) *Casting*: If the i th agent fails to detect information at any
 391 particular instant, then the next state is obtained using
 392 the following relation:

$$393 \quad x_i(t_{h+1}) = \frac{\|x_i(t_h) - x_{s_i}(t_h)\|}{2} + x_{s_i}(t_h). \quad (22)$$

- 394 3) *Search and Exploration*: If all the agents fail to detect
 395 odor clues for a time segment $[t_h, t_{h+l}] > \delta_0$ for some
 396 $l \in \mathbb{N}$ and $\delta_0 \in \mathbb{R}^+$ being the time interval for which
 397 no clues are detected or some constraint on wait time
 398 placed at the start of the experiment, then the next state
 399 is updated as

$$400 \quad x_i(t_{h+1}) = x_{s_i}(t_h) + F_\sigma^\psi. \quad (23)$$

401 In (23), F_σ^ψ is some random parameter with σ as its
 402 standard deviation and ψ as its mean.

403 C. Decentralized Control

404 In the control layer, we design a robust and powerful con-
 405 troller on the paradigms of sliding mode. It is worthy to
 406 mention that based on instantaneous sensing and swarm infor-
 407 mation, at different times, each agent can take up the role of a
 408 virtual leader whose opinion needs to be kept by other agents.
 409 The trajectory is planned by the leader agent based on surging,
 410 casting, and searching behavior. ϕ from (7) has been provided
 411 to the controller as the reference to be tracked. The tracking
 412 error is formulated as

$$413 \quad e_i(t) = x_i(t) - \phi(t_h); t \in [t_h, t_{h+1}]. \quad (24)$$

414 In terms of graph theory, we can reformulate the error
 415 variable as

$$416 \quad \epsilon_i(t) = (\mathcal{L} + \mathcal{B})e_i(t) = (\mathcal{L} + \mathcal{B})(x_i(t) - \phi(t_h)). \quad (25)$$

417 From this point onward, we shall denote $\mathcal{L} + \mathcal{B}$ as \mathcal{H} . Next,
 418 we propose the nonlinear sliding manifold

$$419 \quad s_i(t) = \lambda_1 \tanh(\lambda_2 \epsilon_i(t)) \quad (26)$$

420 which offers faster reachability to the surface. $\lambda_1 \in \mathbb{R}^+$
 421 represents the speed of convergence to the surface, and
 422 $\lambda_2 \in \mathbb{R}^+$ denotes the slope of the nonlinear sliding manifold.

These are coefficient weighting parameters that affect the
 423 system performance. In linear sliding manifolds, the mag-
 424 nitude of error is directly proportional to the magnitude of
 425 control effort needed to maintain sliding motion. In order
 426 to prevent violations of actuator constraints, the control
 427 effort is hard upper and lower bounded by some finite value,
 428 thereby making only a portion of the manifold attractive
 429 (termed as sliding regime). There is no guarantee of desired
 430 performance or stability outside the sliding regime. Moreover,
 431 if the reference state is too far from the current system state
 432 and the actuator saturates, the controller is unable to cope
 433 up, resulting in instability. Hence, it is beneficial to design
 434 nonlinear sliding manifolds that can hold the system states
 435 regardless of their location in the state space. 436

In general, traditional sliding mode controllers suffer from
 437 an undesirable effect of infinite frequency oscillations, known
 438 as chattering [41]. While electronic switching systems may
 439 exploit this phenomenon, mechanical hardware may result in
 440 wear and tear. Many a times, simulations engines used in
 441 numerical analysis and modeling, as well as sampling, switch-
 442 ing and delay caused by hardware used to realize the system
 443 also introduce chattering and result in excitation of unmodeled
 444 high frequency dynamics. This has an adverse effect on system
 445 performance like low control accuracy and different losses in
 446 circuits and system. Techniques to smoothen the control sig-
 447нал by making continuous approximation of the reaching law
 448 via sigmoid functions [44] also exist in literature, but then
 449 there is a tradeoff between performance and chattering. Other
 450 methods to eliminate chattering include use of higher order
 451 sliding mode techniques [45], [46] in which additional hard-
 452 ware is needed to differentiate the control signal. Traditional
 453 reaching laws in the literature of sliding mode [41], [47], [48]
 454 employ a control effort of fixed gain. In order to shorten the
 455 reaching time, a larger control input was designed, leading to
 456 chattering. On the contrary, we have designed the gain to be
 457 nonlinear by using an inverse sine hyperbolic function. This
 458 function is odd and monotonous. Whenever the trajectories are
 459 away from the surface, the gain is high and they are pulled
 460 toward the hyperplane quickly, and when the trajectories are
 461 near the hyperplane, the gain is reduced to avoid chattering.
 462 This variable gain in the reaching law results in a smoother
 463 control signal as opposed to a discontinuous one. Moreover,
 464 interdependence and propinquity of the unwanted chattering
 465 phenomenon with controller gain have been obviated [49] (see
 466 supplementary material, Section III, p. 3). 467

The forcing function has been proposed as

$$468 \quad \dot{s}_i(t) = -\mu \sinh^{-1}(m + w|s_i(t)|) \text{sign}(s_i(t)). \quad (27) \quad 469$$

In (27), m is a small offset such that the argument of $\sinh^{-1}(\cdot)$
 470 function remains nonzero and w is the gain of the controller.
 471 The parameter μ facilitates additional gain tuning. In gen-
 472 eral, $m \ll w$. This novel reaching law contains a nonlinear
 473 gain and provides faster convergence toward the manifold.
 474 Moreover, this reaching law is smooth and chattering free,
 475 which is highly desirable in mechatronic systems to ensure
 476 safe operation. 477

Theorem 1: Given the dynamics of MAS (5) connected in
 478 a directed topology, error candidates (24), (25) and the sliding
 479

480 manifold (26), the stabilizing control law that ensures accurate
481 reference tracking under consensus can be described as

$$482 \quad u_{SM_i}(t) = -\left\{ (\Lambda \mathcal{H})^{-1} \mu \sinh^{-1}(m + w|s_i(t)|) \text{sign}(s_i(t)) \Gamma^{-1} \right. \\ 483 \quad \left. + (f(x_i(t)) - \dot{\phi}(t_h)) \right\} \quad (28)$$

484 where $\Lambda = \lambda_1 \lambda_2$, $\Gamma = 1 - \tanh^2(\lambda_2 \epsilon_i(t))$, $w > \sup_{t \geq 0} \{\|\zeta_i\|\}$
485 & $\mu > \sup\{\|\Lambda \mathcal{H} \zeta_i \Gamma\|\}$.

486 *Remark 4:* As mentioned earlier, $\lambda_1, \lambda_2 \in \mathbb{R}^+$. This ensures
487 $\Lambda \neq 0$ and hence its nonsingularity. The argument of $\tanh(\cdot)$
488 is always finite and satisfies $\lambda_2 \epsilon_i(t) \neq \pi \iota(\kappa + 1/2)$ for $\kappa \in \mathbb{Z}$,
489 thus Γ is also invertible. Moreover, the nonsingularity of \mathcal{H}
490 can be established directly if the digraph contains a spanning
491 tree with leader agent as a root.

492 *Proof:* From (25) and (26), we can write

$$493 \quad \dot{s}_i(t) = \lambda_1 \left\{ \lambda_2 \dot{\epsilon}_i(t) \left(1 - \tanh^2(\lambda_2 \epsilon_i(t)) \right) \right\} \quad (29)$$

$$494 \quad = \lambda_1 \lambda_2 \dot{\epsilon}_i(t) - \lambda_1 \lambda_2 \dot{\epsilon}_i(t) \tanh^2(\lambda_2 \epsilon_i(t)) \quad (30)$$

$$495 \quad = \lambda_1 \lambda_2 \dot{\epsilon}_i(t) \left\{ 1 - \tanh^2(\lambda_2 \epsilon_i(t)) \right\} \quad (31)$$

$$496 \quad = \Lambda \mathcal{H} (\dot{x}_i(t) - \dot{\phi}(t_h)) \Gamma \quad (32)$$

497 with Λ and Γ as defined in Theorem 1. From (5), (32) can be
498 further simplified as

$$499 \quad \dot{s}_i(t) = \Lambda \mathcal{H} (f(x_i(t)) + u_{SM_i}(t) + \zeta_i - \dot{\phi}(t_h)) \Gamma. \quad (33)$$

500 Using (27), the control that brings the state trajectories on to
501 the sliding manifold can now be written as

$$502 \quad u_{SM_i}(t) = -\left\{ (\Lambda \mathcal{H})^{-1} \mu \sinh^{-1}(m + w|s_i(t)|) \text{sign}(s_i(t)) \Gamma^{-1} \right. \\ 503 \quad \left. + (f(x_i(t)) - \dot{\phi}(t_h)) \right\}$$

504 which is same as (28), thereby completing the proof. ■

505 *Remark 5:* The control (28) can be practically implemented
506 as it does not contain the uncertainty term.

507 It is crucial to analyze the necessary and sufficient conditions
508 for the existence of sliding mode when control protocol
509 col (28) is used. We regard the system to be in sliding mode
510 if for any time $t_1 \in [0, \infty)$, system trajectories are brought
511 upon the manifold $s_i(t) = 0$ and are constrained there for all
512 time thereafter, i.e., for $t \geq t_1$, sliding motion occurs.

513 *Theorem 2:* Consider the system described by (5), error
514 candidates (24), (25), sliding manifold (26), and the control
515 protocol (28). Sliding mode is said to exist in vicinity of sliding
516 manifold, if the manifold is attractive, i.e., trajectories
517 emanating outside it continuously decrease toward it. Stating
518 alternatively, reachability to the surface is ensured for some
519 reachability constant $\eta > 0$. Further, stability can be guaranteed
520 in the sense of Lyapunov if gain μ is designed as
521 $\mu > \sup\{\|\Lambda \mathcal{H} \zeta_i \Gamma\|\}$.

522 *Proof:* Let us take into account, a Lyapunov function
523 candidate

$$524 \quad V_i = 0.5 s_i^2. \quad (34)$$

525 Taking derivative of (34) along system trajectories yield

$$526 \quad \dot{V}_i = s_i \dot{s}_i \quad (35)$$

$$527 \quad = s_i \{ \Lambda \mathcal{H} (f(x_i(t)) + u_{SM_i}(t) + \zeta_i - \dot{\phi}(t_h)) \Gamma \}. \quad (36)$$

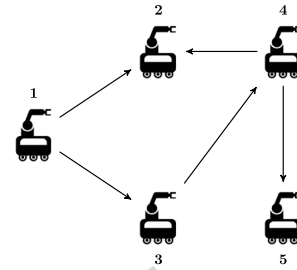


Fig. 2. Topology in which agents are connected.

Substituting the control protocol (28) in (36), we have

$$\begin{aligned} \dot{V}_i &= s_i \left(-\mu \sinh^{-1}(m + w|s_i|) \text{sign}(s_i) + \Lambda \mathcal{H} \zeta_i \Gamma \right) \\ &= -\mu \sinh^{-1}(m + w|s_i|) \|s_i\| + \Lambda \mathcal{H} \zeta_i \Gamma \|s_i\| \\ &= \left\{ -\mu \sinh^{-1}(m + w|s_i|) + \Lambda \mathcal{H} \zeta_i \Gamma \right\} \|s_i\| \\ &= -\eta \|s_i\| \end{aligned} \quad (37)$$

where $\eta = \mu \sinh^{-1}(m + w|s_i|) - \Lambda \mathcal{H} \zeta_i \Gamma > 0$ is called
reachability constant. For $\mu > \sup\{\|\Lambda \mathcal{H} \zeta_i \Gamma\|\}$, we have

$$\dot{V}_i < 0. \quad (38)$$

Thus, the derivative of Lyapunov function candidate is negative
definite confirming stability in the sense of Lyapunov.

Since, $\mu > 0$, $\|s_i\| > 0$ and $\sinh^{-1}(\cdot) > 0$ due to the nature
of its arguments. Therefore, (27) and (37) together provide
implications that $\forall s_i(0)$, $s_i \dot{s}_i < 0$ and the surface is globally
attractive. This completes the proof. ■

V. RESULTS AND DISCUSSIONS

Fig. 2 depicts the interaction topology of the agents [8] as
a digraph. In theory, the control has been synthesized using
 \mathcal{H} matrix. If the elements of \mathcal{H} are constant, the topology is
fixed, and if the elements of \mathcal{H} are time-varying, the connection
represents a switching topology. Note that although the
developed theory and hierarchical scheme can be extended to
a switching topology as well, we shall simplify the case by
taking a fixed topology.

Assumption 5: Agent 1 appears as the virtual leader to all
other agents. Therefore, the topology is fixed and directed.

The associated graph matrices have been described as

$$\mathcal{A} = \begin{bmatrix} 0 & 0 & 1 & 0 \\ 0 & 0 & 0 & 0 \\ 0 & 1 & 0 & 0 \\ 0 & 0 & 1 & 0 \end{bmatrix}, \quad \mathcal{B} = \begin{bmatrix} 1 & 0 & 0 & 0 \\ 0 & 1 & 0 & 0 \\ 0 & 0 & 0 & 0 \\ 0 & 0 & 0 & 0 \end{bmatrix} \quad (554)$$

$$\mathcal{D} = \begin{bmatrix} 1 & 0 & 0 & 0 \\ 0 & 0 & 0 & 0 \\ 0 & 0 & 1 & 0 \\ 0 & 0 & 0 & 1 \end{bmatrix} \quad (555)$$

$$\mathcal{L} = \mathcal{D} - \mathcal{A} = \begin{bmatrix} 1 & 0 & -1 & 0 \\ 0 & 0 & 0 & 0 \\ 0 & -1 & 1 & 0 \\ 0 & 0 & -1 & 1 \end{bmatrix} \quad (556)$$

$$\mathcal{L} + \mathcal{B} = \begin{bmatrix} 2 & 0 & -1 & 0 \\ 0 & 1 & 0 & 0 \\ 0 & -1 & 1 & 0 \\ 0 & 0 & -1 & 1 \end{bmatrix}. \quad (39) \quad (557)$$

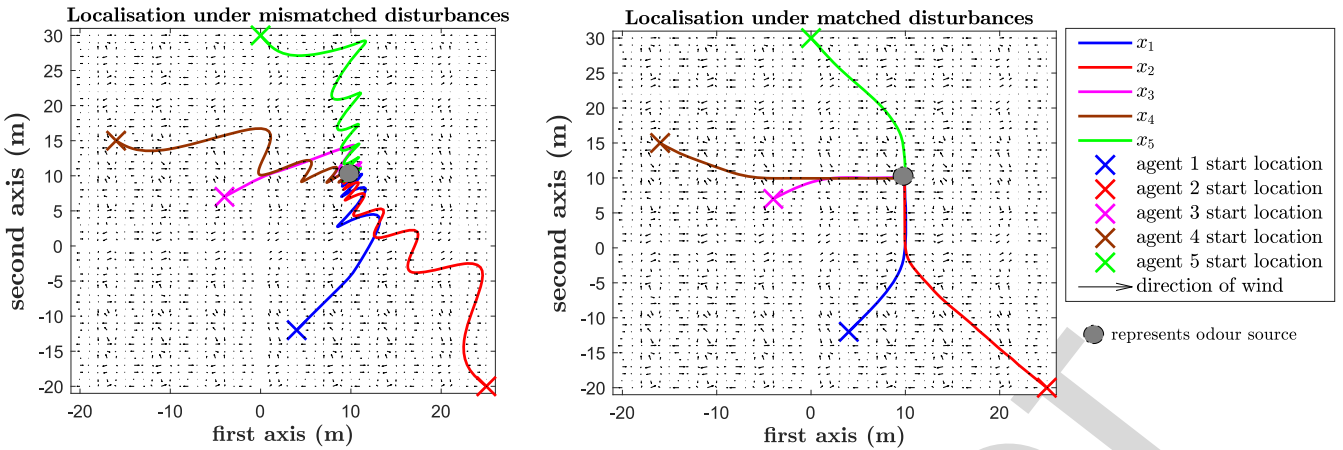


Fig. 3. Localization by MAS under the effect of mismatched and matched disturbances.

TABLE I
VALUES OF THE DESIGN PARAMETERS USED IN SIMULATION

k_1	ω_{max}	α_1	α_2	λ_1	λ_2	μ	m	w
0.5	2 rad/s	0.25	0.25	1.774	2.85	5	10^{-3}	2

TABLE II
FOUR CASES OF LOCALIZATION CONSIDERED IN THIS PAPER

Technique	Consensus	Formation	Matched perturbations	Mismatched perturbations
Case 1	✓	✗	✓	✗
Case 2	✗	✓	✓	✗
Case 3	✓	✗	✗	✓
Case 4	✗	✓	✗	✓

558 Dynamics of the agents are described as

$$\dot{x}_1 = 0.1\sqrt{3}\sin(x_1) + \cos(2\pi t) + u_{SM_1}(t) + \varsigma_1 \quad (40)$$

$$\dot{x}_2 = 0.1\sin(x_2) - \cos(e^{-x_2 t}) + u_{SM_2}(t) + \varsigma_2 \quad (41)$$

$$\dot{x}_3 = 0.1\sqrt{3}\sin(x_3) + \cos^2(2\pi t) + u_{SM_3}(t) + \varsigma_3 \quad (42)$$

$$\dot{x}_4 = 0.1\sin(x_4) + \cos(x_4) + u_{SM_4}(t) + \varsigma_4 \quad (43)$$

$$\dot{x}_5 = 0.1\cos(x_5) - \cos(2\pi t) - e^{-t} + u_{SM_5}(t) + \varsigma_5. \quad (44)$$

564 Initial conditions have been chosen to be far from the equi-
565 librium point. We shall consider a time varying disturbance
566 $\varsigma_i = 0.3\sin(\pi^2 t^2)$ for matched case and $\varsigma_i = 20\sin(\pi^2 t^2)$
567 for mismatched (or, unmatched) case, accuracy parameter
568 $\theta = 0.001$ and maximum mean airflow velocity $\bar{v}_{a_{max}} = 1$ m/s.
569 Other key design parameters are provided in Table I.

570 Turbulence coefficient, K , is taken to be 0.02 m²/s and fila-
571 ment release rate, $q_0 = 2$ mg/s of diffusing substance. We
572 shall present the results for both the cases of localization
573 in \mathbb{R}^1 and \mathbb{R}^2 to demonstrate the efficiency of the designed
574 control scheme.

575 For the case of \mathbb{R}^1 , the odor source is randomly placed
576 between 10 and 11 m (see supplementary material, Section II
577 for illustrations). Agents start from various initial conditions
578 that are far from the origin and progress toward the source
579 via instantaneous plume sensing (by sensing odor molecules,
580 or filaments). As soon as the leader agent senses the odor

581 molecules, the information of predicted next state is exchanged
582 among other agents. This local information is then used to
583 make a consensus while localization. Agents come to con-
584 sensus in finite time to locate the odor source. In spite of
585 time varying disturbance, the plume tracking is accurate and
586 the localization is successful. Filaments or odor molecules
587 (source information) are released from the odor source and are
588 detected by the sensors equipped with the agents. The tracking
589 controller attempts to minimize the error between the predicted
590 next state and the actual next state. The tracking error lies in
591 the close vicinity of zero as expected, implying that the track-
592 ing error has almost been nullified. Norm of tracking errors
593 in \mathbb{R}^1 has been depicted in Fig. 4 to depict near nullification
594 of error. Novel sliding manifolds, designed in this paper, also
595 come to consensus in very short span of time, as evident from
596 Fig. 5. It is, then, quite clear that the convergence of state
597 trajectories to the sliding manifold is very fast and is highly
598 desired to ensure a high degree of robustness and autonomy.
599 Such manifolds can also be utilized to attain a desired con-
600 vergence speed by simple tuning of design parameters. Use
601 of a novel inverse sine hyperbolic reaching law results in a
602 smooth control signals for all the agents. The use of smooth
603 sliding mode controller ensures safe operation in mechatronic
604 devices. Fig. 6 depicts the control signals of all the agents
605 when localization is carried in \mathbb{R}^1 . It is clear that the signal is
606 chattering free, smooth, and accurate.

Having discussed the case of \mathbb{R}^1 , we shall now discuss
607 localization in \mathbb{R}^2 . To avoid confusion between state vari-
608 able x and axis labeled as x in the usual sense, we have
609 adopted to refer abscissa as first axis and ordinate as second
610 axis throughout this discussion. Agents are driven into consen-
611 sus to locate the odor source in \mathbb{R}^2 in the domain described
612 by the axis limits. Within the domain of localization, a total
613 of 25 trials were done with various initial conditions cho-
614 sen far from the origin. Fig. 7 shows the average time spent
615 in four cases—localization via consensus under matched per-
616 turbations (case 1), localization via formation under matched
617 perturbations (case 2), localization via consensus under mis-
618 matched perturbations (case 3), and localization via formation
619 under mismatched perturbations (case 4). Similar to the results
620 in [50], the success rate of this technique is also 100% except
621

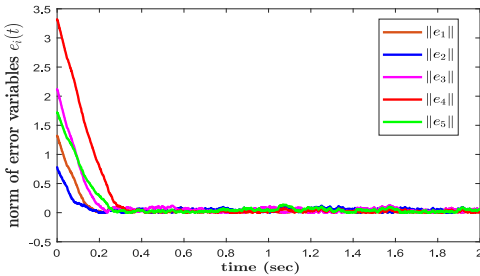
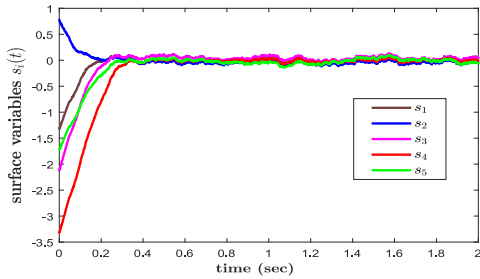
Fig. 4. Localization tracking errors in \mathbb{R}^1 .

Fig. 5. Sliding manifolds during consensus.

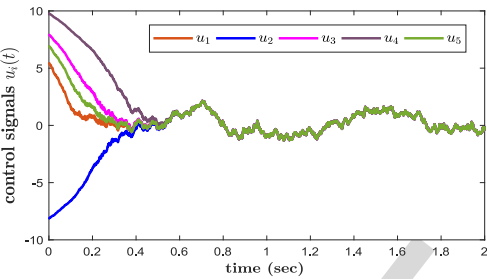


Fig. 6. Smooth control signals of all the agents during consensus.

for the fact that time spent in localization is lesser via this technique owing to faster convergence of state trajectories to the sliding manifold. The four cases have been illustrated here in a tabular format for ease of reference. A check (cross) mark in a particular column indicates that the particular strategy has been used (not used) in localization.

We shall also present two cases under which localization has been tasked: 1) under consensus and 2) under parallel formation. Note that agents may be subjected to any geometrical pattern, or formation that deems suitable for the task at hand. In Figs. 8 and 9, norms of tracking errors along first and second axis have been depicted. Similar to the error profile in Fig. 4, the tracking is accurate and the agents are able to complete the localization task in finite time. For a random trial, Fig. 3 shows localization in a turbulent environment under the effect of both mismatched and matched disturbances. Under mismatched disturbances and turbulence, localization takes slightly more time as compared with its matched disturbance counterpart. The domain for this task has been set to be a grid of 50×50 along both the axes. Abscissa ranges from -20 to 30 , and so does the ordinate. Start position of agents are denoted by a “ \times ” in five different colors. Filaments or the odor molecules are released from the odor source and

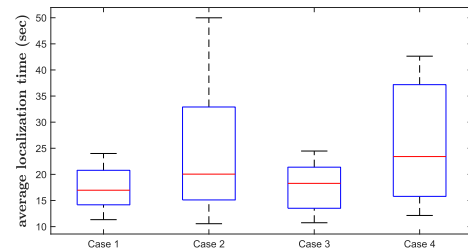


Fig. 7. Average localization time for 25 trials.

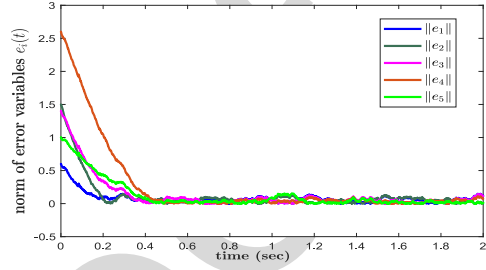


Fig. 8. Localization tracking errors along first axis.

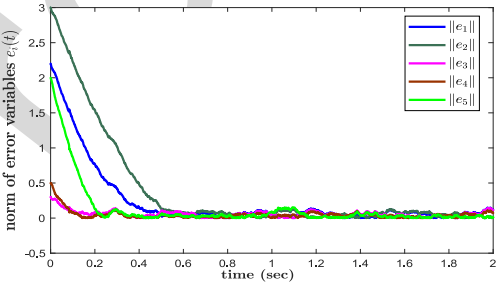


Fig. 9. Localization tracking errors along second axis.

TABLE III
PERFORMANCE METRICS IN CONTEXT OF LOCALIZATION

Technique	Average Success rate	Median localisation Time	Control Implementation
Case 1 (this study)	100%	16 sec	Time-triggered
Case 2 (this study)	100%	20 sec	Time-triggered
Case 3 (this study)	100%	18 sec	Time-triggered
Case 4 (this study)	100%	22 sec	Time-triggered
PSO [33]	21.5%	986.25 sec	Time-triggered
FTMCS [50]	100%	137.5 sec	Time-triggered

the molecules disperse in the domain characterized by heavy turbulence. Performance metrics of localization in terms of average time spent in locating the source of odor have been provided in Table III. For best case scenario of localization in \mathbb{R}^2 , please refer the supplementary material, Section II.

Finally, we state some limitations of the current approach. If the domain of localization is very large, the number of agents should increase in order to effectively solve OSL problem. However, increase in number of agents shall add to the economy, and there is a cost to maintain the communication links. Further, anomalies such as packet dropout, link failure, and latencies in communication should be carefully checked. Another scenario where localization is quite difficult, if not impossible, is the presence of multiple time varying global maxima and local minima. This shall render MAS slightly confused and a different approach should be adopted, such as

extrapolating the location based on known (or probable) presence of the source. All these issues shall be addressed in our future studies sequentially.

VI. CONCLUSION

In this paper, odor source localization via multiagent systems has been addressed. The localizing task is based on a cooperative strategy where agents interact locally among themselves to locate the source of odor in finite time. A hierarchical control scheme has been developed to predict the probable location of odor source using information of wind and concentration. This control scheme based on PSO and SMC is robust and insensitive to matched disturbances. Numerical simulations demonstrate the effectuality of the proposed scheme for both cases 1) when agents localize the odor source via consensus and 2) parallel formation. The localization takes very less time compared to other strategies and the success rate is 100%. In future, we shall address the communication issues associated with the problem.

COMPETING INTERESTS

The authors declare that there are no competing interests associated with this paper.

REFERENCES

- [1] G. S. Settles, "Sniffers: Fluid-dynamic sampling for olfactory trace detection in nature and homeland security—The 2004 freeman scholar lecture," *J. Fluids Eng.*, vol. 127, no. 2, pp. 189–218, Feb. 2005, doi: [10.1115/1.1891146](https://doi.org/10.1115/1.1891146).
- [2] D. W. Gage, "Many-robot MCM search systems," in *Proc. Auton. Veh. Mine Countermeas. Symp.*, 1995, pp. 9–55.
- [3] H. Ishida, T. Nakamoto, T. Moriizumi, T. Kikas, and J. Janata, "Plume-tracking robots: A new application of chemical sensors," *Biol. Bull.*, vol. 200, no. 2, pp. 222–226, 2001. [Online]. Available: <https://doi.org/10.2307/1543320>
- [4] V. Formisano, S. Atreya, T. Encrenaz, N. Ignatiev, and M. Giuranna, "Detection of methane in the atmosphere of Mars," *Science*, vol. 306, no. 5702, pp. 1758–1761, 2004. [Online]. Available: <http://science.sciencemag.org/content/306/5702/1758>
- [5] V. A. Krasnopolsky, J. P. Maillard, and T. C. Owen, "Detection of methane in the martian atmosphere: Evidence for life?" *Icarus*, vol. 172, no. 2, pp. 537–547, 2004. [Online]. Available: <http://www.sciencedirect.com/science/article/pii/S0019103504002222>
- [6] J. A. Farrell, S. Pang, and W. Li, "Plume mapping via hidden Markov methods," *IEEE Trans. Syst., Man, Cybern. B, Cybern.*, vol. 33, no. 6, pp. 850–863, Dec. 2003.
- [7] M. Vergassola, E. Villermoux, and B. Shraiman, "'Infotaxis' as a strategy for searching without gradients," *Nature*, vol. 445, no. 7126, pp. 406–409, 2007. [Online]. Available: <https://hal.archives-ouvertes.fr/hal-00326807>
- [8] A. Sinha, R. Kaur, R. Kumar, and A. P. Bhondekar, "Cooperative control of multi-agent systems to locate source of an odor," *ArXiv e-prints*, Nov. 2017.
- [9] X. Cui, C. T. Hardin, R. K. Ragade, and A. S. Elmaghriby, "A swarm approach for emission sources localization," in *Proc. 16th IEEE Int. Conf. Tools Artif. Intell.*, Nov. 2004, pp. 424–430.
- [10] C. Lytridis, G. S. Virk, Y. Rebour, and E. E. Kadar, "Odor-based navigational strategies for mobile agents," *Adapt. Behav.*, vol. 9, nos. 3–4, pp. 171–187, Apr. 2001, doi: [10.1177/10597123010093004](https://doi.org/10.1177/10597123010093004).
- [11] R. Rozas, J. Morales, and D. Vega, "Artificial smell detection for robotic navigation," in *Proc. 5th Int. Conf. Adv. Robot. Unstruct. Environ. (ICAR)*, vol. 2, Jun. 1991, pp. 1730–1733.
- [12] V. Genovese, P. Dario, R. Magni, and L. Odetti, "Self organizing behavior and swarm intelligence in a pack of mobile miniature robots in search of pollutants," in *Proc. IEEE/RSJ Int. Conf. Intell. Robots Syst.*, vol. 3, Jul. 1992, pp. 1575–1582.
- [13] L. Buscemi, M. Prati, and G. Sandini, "Cellular robotics: Behaviour in polluted environments," in *Proc. 2nd Int. Symp. Distrib. Auton. Robot. Syst.*, 1994.
- [14] M. H. E. Larcombe, *Robotics in Nuclear Engineering: Computer Assisted Teleoperation in Hazardous Environments With Particular Reference to Radiation Fields*, Graham and Trotman, Inc., 1984.
- [15] R. Russell, "Chemical source location and the RoboMole project," in *Proc. Aust. Robot. Autom. Assoc.*, 2003, pp. 1–6.
- [16] R. A. Russell, "Locating underground chemical sources by tracking chemical gradients in 3 dimensions," in *Proc. IEEE/RSJ Int. Conf. Intell. Robots Syst. (IROS)*, vol. 1, Sep. 2004, pp. 325–330.
- [17] R. A. Russell, "Robotic location of underground chemical sources," *Robotica*, vol. 22, no. 1, pp. 109–115, 2004.
- [18] D. Martinez, L. Perrinet, and D. Walther, "Cooperation between vision and olfaction in a koala robot," in *Proc. Workshop Rep. Neuromorphic Eng.*, 2002, pp. 51–53.
- [19] A. Loutfi, S. Coradeschi, L. Karlsson, and M. Broxvall, "Putting olfaction into action: Using an electronic nose on a multi-sensing mobile robot," in *Proc. IEEE/RSJ Int. Conf. Intell. Robots Syst. (IROS)*, vol. 1, Sep. 2004, pp. 337–342.
- [20] H. Ishida, K. Yoshikawa, and T. Moriizumi, "Three-dimensional gas-plume tracking using gas sensors and ultrasonic anemometer," in *Proc. IEEE Sensors*, vol. 3, Oct. 2004, pp. 1175–1178.
- [21] R. A. Russell, A. Bab-Hadiashar, R. L. Shepherd, and G. G. Wallace, "A comparison of reactive robot chemotaxis algorithms," *Robot. Auton. Syst.*, vol. 45, no. 2, pp. 83–97, 2003. [Online]. Available: <http://www.sciencedirect.com/science/article/pii/S0921889003001209>
- [22] S. Pang and J. A. Farrell, "Chemical plume source localization," *IEEE Trans. Syst., Man, Cybern. B, Cybern.*, vol. 36, no. 5, pp. 1068–1080, Oct. 2006.
- [23] D. Zarzhitsky, "Physics-based approach to chemical source localization using mobile robotic swarms," Ph.D. dissertation, Dept. Comput. Sci., Univ. Wyoming, Laramie, WY, USA, 2008.
- [24] V. Braithwaite, *Vehicles: Experiments in Synthetic Psychology*. Boston, MA, USA: MIT Press, 1984.
- [25] H. Ishida, K. Suetsugu, T. Nakamoto, and T. Moriizumi, "Study of autonomous mobile sensing system for localization of odor source using gas sensors and anemometric sensors," *Sensors Actuators A Phys.*, vol. 45, no. 2, pp. 153–157, 1994. [Online]. Available: <http://www.sciencedirect.com/science/article/pii/0924424794008299>
- [26] L. Marques and A. T. D. Almeida, "Electronic nose-based odour source localization," in *Proc. 6th Int. Workshop Adv. Motion Control*, Apr. 2000, pp. 36–40.
- [27] L. Marques, U. Nunes, and A. T. de Almeida, "Olfaction-based mobile robot navigation," *Thin Solid Films*, vol. 418, no. 1, pp. 51–58, 2002. [Online]. Available: <http://www.sciencedirect.com/science/article/pii/S004060900200593X>
- [28] C. W. Reynolds, "Flocks, herds and schools: A distributed behavioral model," *SIGGRAPH Comput. Graph.*, vol. 21, no. 4, pp. 25–34, Aug. 1987. [Online]. Available: <http://doi.acm.org/10.1145/37402.37406>
- [29] W. Ren and R. W. Beard, "Consensus seeking in multiagent systems under dynamically changing interaction topologies," *IEEE Trans. Autom. Control*, vol. 50, no. 5, pp. 655–661, May 2005.
- [30] R. Olfati-Saber, J. A. Fax, and R. M. Murray, "Consensus and cooperation in networked multi-agent systems," *Proc. IEEE*, vol. 95, no. 1, pp. 215–233, Jan. 2007.
- [31] W. Yu, G. Chen, W. Ren, J. Kurths, and W. X. Zheng, "Distributed higher order consensus protocols in multiagent dynamical systems," *IEEE Trans. Circuits Syst. I, Reg. Papers*, vol. 58, no. 8, pp. 1924–1932, Aug. 2011.
- [32] A. T. Hayes, A. Martinoli, and R. M. Goodman, "Swarm robotic odor localization: Off-line optimization and validation with real robots," *Robotica*, vol. 21, no. 4, pp. 427–441, Aug. 2003, doi: [10.1017/S0263574703004946](https://doi.org/10.1017/S0263574703004946).
- [33] L. Marques, U. Nunes, and A. T. de Almeida, "Particle swarm-based olfactory guided search," *Auton. Robots*, vol. 20, no. 3, pp. 277–287, Jun. 2006. [Online]. Available: <https://doi.org/10.1007/s10514-006-7567-0>
- [34] J. Kennedy and R. Eberhart, "Particle swarm optimization," in *Proc. IEEE Int. Conf. Neural Netw.*, vol. 4, Nov. 1995, pp. 1942–1948.
- [35] W. Jatmiko, K. Sekiyama, and T. Fukuda, "A PSO-based mobile robot for odor source localization in dynamic advection-diffusion with obstacles environment: Theory, simulation and measurement," *IEEE Comput. Intell. Mag.*, vol. 2, no. 2, pp. 37–51, May 2007.
- [36] Q. Lu, S.-R. Liu, and X.-N. Qiu, "A distributed architecture with two layers for odor source localization in multi-robot systems," in *Proc. IEEE Congr. Evol. Comput.*, Jul. 2010, pp. 1–7.

- AQ8
- 801 [37] Q. Lu and Q.-L. Han, "Decision-making in a multi-robot system for odor
802 source localization," in *Proc. 37th Annu. Conf. IEEE Ind. Electron. Soc.*
803 (*IECON*), Nov. 2011, pp. 74–79.
804 [38] Q. Lu, S. Liu, X. Xie, and J. Wang, "Decision making and finite-time
805 motion control for a group of robots," *IEEE Trans. Cybern.*, vol. 43,
806 no. 2, pp. 738–750, Apr. 2013.
807 [39] J. A. Farrell, J. Murlis, X. Long, W. Li, and R. T. Cardé,
808 "Filament-based atmospheric dispersion model to achieve short
809 time-scale structure of odor plumes," *Environ. Fluid Mech.*,
810 vol. 2, no. 1, pp. 143–169, Jun. 2002. [Online]. Available:
811 <https://doi.org/10.1023/A:1016283702837>
812 [40] F. R. K. Chung, "Spectral graph theory," in *Proc. CBMS Reg. Conf. Math.*,
813 vol. 92, 1997. [Online]. Available: <http://bookstore.ams.org/cbms-92>
814 [41] K. D. Young, V. I. Utkin, and U. Ozguner, "A control engineer's guide
815 to sliding mode control," *IEEE Trans. Control Syst. Technol.*, vol. 7,
816 no. 3, pp. 328–342, May 1999.
817 [42] M. L. Cao, Q. H. Meng, Y. X. Wu, M. Zeng, and W. Li, "Consensus
818 based distributed concentration-weighted summation algorithm for gas-
819 leakage source localization using a wireless sensor network," in
820 *Proc. 32nd Chin. Control Conf.*, Jul. 2013, pp. 7398–7403.
821 [43] J. Matthes, L. Groll, and H. B. Keller, "Source localization by spatially
822 distributed electronic noses for advection and diffusion," *IEEE Trans. Signal Process.*,
823 vol. 53, no. 5, pp. 1711–1719, May 2005.
824 [44] A. Sinha and R. K. Mishra, "Nonlinear autonomous altitude control
825 of a miniature helicopter UAV based on sliding mode methodology,"
826 *Int. J. Electron. Commun. Technol.*, vol. 6, no. 1, pp. 32–37,
827 Mar. 2015. [Online]. Available: <http://www.iject.org/C2E2-2015/7-Abhinav-Sinha.pdf>
828 [45] A. Msaddek, A. Gaaloul, and F. M'sahli, *Output Feedback Robust
829 Exponential Higher Order Sliding Mode Control*. Singapore: Springer,
830 2017, pp. 53–72.
831 [46] F. Plestan, V. Brégeault, A. Glumineau, Y. Shtessel, and E. Moulay,
832 *Advances in High Order and Adaptive Sliding Mode Control—Theory
833 and Applications*. Heidelberg, Germany: Springer, 2012, pp. 465–492.
834 [47] A. Sinha and R. K. Mishra, "Control of a nonlinear continuous
835 stirred tank reactor via event triggered sliding modes," *Chem. Eng. Sci.*,
836 vol. 187, pp. 52–59, Sep. 2018. [Online]. Available:
837 <http://www.sciencedirect.com/science/article/pii/S0009250918302719>
838 [48] C. Edwards and S. K. Spurgeon, *Sliding Mode Control: Theory and
839 Applications*. London, U.K.: CRC Press, 1998.
840 [49] T. Majumder, R. K. Mishra, A. Sinha, S. S. Singh, and
841 P. K. Sahu, "Congestion control in cognitive radio networks with
842 event-triggered sliding mode," *AEU Int. J. Electron. Commun.*,
843 vol. 90, pp. 155–162, Jun. 2018. [Online]. Available:
844 <https://www.sciencedirect.com/science/article/pii/S1434841117325438>
845 [50] Q. Lu, Q. L. Han, X. Xie, and S. Liu, "A finite-time motion control strategy
846 for odor source localization," *IEEE Trans. Ind. Electron.*, vol. 61,
847 no. 10, pp. 5419–5430, Oct. 2014.



850 **Abhinav Sinha** received the B.Tech. degree in
851 electronics and instrumentation engineering from
852 the Kalinga Institute of Industrial Technology,
853 Bhubaneswar, India, in 2014 and the M.Tech.
854 degree in mechatronics from the Indian Institute of
855 Engineering Science and Technology, Shibpur, India,
856 in 2018.

857 He is currently a Doctoral Researcher with
858 the Dynamics and Control Group, Department
859 of Aerospace Engineering, Indian Institute of
860 Technology Bombay, Mumbai, India. He was an
861 Assistant System Engineer with the Engineering and Industrial Services
862 Division, Tata Consultancy Services (TCS) Ltd., Mumbai, from 2014 to 2016,
863 where he researched on control system integration, manufacturing execu-
864 tion systems, enterprise manufacturing intelligence, network segmentation,
865 data integration, and data security at plant level. He was also a Visiting
866 Faculty with TCS Global Learning Centre, India, in 2015. From 2017 to
867 2018, he was a Graduate Researcher with CSIR-Central Scientific Instruments
868 Organisation, Chandigarh, India, where he researched for his master's degree.
869 His current research interests include sliding mode control, event-based con-
870 trol, multiagent systems, cooperative control, and cyber-physical systems.

871 Mr. Sinha was a recipient of the IEEE Best Paper Award (IEEE Pune
872 Section & IEEE Computer Society) in 2015, On the Spot Award (TCS) in
873 2015, and the Champions of Initial Learning Programme (TCS) in 2015.
874 He is a member of the International Federation of Automatic Control,
875 Automatic Control and Dynamical Optimization Society, and the Asian
876 Control Association. He currently serves as a Reviewer for *Nonlinear
877 Dynamics* (Springer) and *IET Generation, Transmission and Distribution*.



878 **Ritesh Kumar** received the B.E. degree in com-
879 puter science and engineering from the Manipal
880 Institute of Technology, Manipal, India, in 2009 and
881 the M.Tech. degree in advanced instrumentation and
882 the Ph.D. degree from the Academy of Scientific &
883 Innovative Research, New Delhi, India, in 2011 and
884 2017, respectively.

885 Since 2011, he has been a Scientist with CSIR-
886 Central Scientific Instruments Organisation (CSIR-
887 CSIO), Chandigarh, India, working on a number of
888 government and industry-sponsored projects involv-
889 ing various domains of information and communication technology. At
890 CSIR-CSIO, he is also responsible for supervising laboratory and tutorials on
891 machine learning. He has authored and co-authored multiple journal papers.
892 His current research interests include big data analytics, perception modeling,
893 and artificial intelligence.

894 Mr. Kumar is a member of Digital Olfaction Society and the Institution of
895 Electronics and Telecommunication Engineers.



896 **Rishemjit Kaur** received the B.E. degree in elec-
897 tronics (instrumentation and control) from Thapar
898 University, Patiala, India, in 2009 and the M.Tech.
899 degree in advanced instrumentation and the Ph.D.
900 degree from the Academy of Scientific & Innovative
901 Research, New Delhi, India, in 2011 and 2017,
902 respectively.

903 She was a Research Scholar with Nagoya
904 University, Nagoya, Japan, from 2014 to 2016. Since
905 2011, she has been a Scientist with CSIR-Central
906 Scientific Instruments Organisation, Chandigarh,
907 India. She received Japanese Government scholarship for research students
908 (MEXT) from 2014 to 2016. Her current research interests include evolution-
909 ary optimization techniques, big data analytics, social network analysis, and
910 machine learning.

911 Dr. Kaur was a recipient of the Genetic and Evolutionary Computation
912 Conference Virtual Creatures Award for her research on developing controller
913 for soft-bodied robots.



914 **Amol P. Bhondekar** received the Ph.D. degree
915 in engineering from Panjab University, Chandigarh,
916 India.

917 He is with CSIR-Central Scientific Instruments
918 Organisation, Chandigarh, where he is a Principal
919 Scientist and the Head of the Department of
920 Agrionics (Post Harvest Technologies). He is also an
921 Associate Professor with the Academy of Scientific
922 and Innovative Research, New Delhi, India. He has
923 number of research articles in reputed journals to his
924 credit. His current research interests include sensors,
925 development of techniques for artificial organoleptics.

926 Dr. Bhondekar is a fellow of the Institution of Electronics and
927 Telecommunication Engineers.

AUTHOR QUERIES

AUTHOR PLEASE ANSWER ALL QUERIES

PLEASE NOTE: We cannot accept new source files as corrections for your paper. If possible, please annotate the PDF proof we have sent you with your corrections and upload it via the Author Gateway. Alternatively, you may send us your corrections in list format. You may also upload revised graphics via the Author Gateway.

AQ1: Author: Please confirm or add details for any funding or financial support for the research of this article.

AQ2: Please provide the department name and postal code for “Indian Institute of Technology Bombay, Mumbai, India” and “CSIR–Central Scientific Instruments Organisation, Chandigarh, India.”

AQ3: Please cite “Table II” inside the text.

AQ4: Figs. 4 and 9 are cited before Fig. 3. Please check if Fig. 3 can be cited earlier, or if Figs. 3–9 can be renumbered so that they are cited in sequential order.

AQ5: Please provide the complete details and exact format for Reference [8].

AQ6: Please provide the page range for References [13] and [40].

AQ7: Please provide the publisher location for Reference [14].

AQ8: Please confirm if the location and publisher information for Reference [45] and [46] is correct as set.

Consensus-Based Odor Source Localization by Multiagent Systems

Abhinav Sinha^{ID}, Ritesh Kumar, Rishemjit Kaur, and Amol P. Bhondekar

Abstract—This paper presents an investigation of the task of localizing unknown source of an odor by heterogeneous multiagent systems. A hierarchical cooperative control strategy has been proposed as a potential candidate to solve the problem. The agents are driven into consensus as soon as the information about the location of source is acquired. The controller has been designed in a hierarchical manner of group decision making, agent path planning, and robust control. In group decision making, particle swarm optimization algorithm has been used along with the information of the movement of odor molecules to predict the odor source location. Next, a trajectory has been mapped using this predicted location of source, and the information is passed to the control layer. A variable structure control has been used in the control layer due to its inherent robustness and disturbance rejection capabilities. Cases of movement of agents toward the source under consensus, and parallel formation have been discussed. The efficacy of the proposed scheme has been confirmed by simulations.

Index Terms—Decentralized cooperative control, heterogeneous multiagent systems (MASs), inverse sine hyperbolic reaching law, odor source localization (OSL), robot olfaction, sliding mode control (SMC).

I. INTRODUCTION

RESEARCH in robot olfaction has received wide attention to address many challenges, some of which include detection of hazardous gases in mines, tunnels and industrial setup, search and rescue of victims, forest fire detection and firefighting [1]–[3], etc. Recently, extra-terrestrial odor source localization via autonomous agents has been carried out on Mars [4], [5]. Numerous simple and complex algorithms for olfaction problems have imitated behavior of biological entities, such as mate seeking by moths, foraging by lobsters, prey tracking by mosquitoes and blue crabs, etc. However, techniques like probabilistic inference [6], [7]; robust control [8]; swarm intelligence [9]; biased random walk [10]; and

optimization and meta-heuristics prove better in localization than aforementioned techniques.

Works on OSL in early 90s were mostly targeted via chemical gradient-based techniques in a diffusion dominated environment [11]–[14]. Attributed to geometry and dimensions of the above-ground agents, this assumption leads to suboptimal performance. This assumption, however, yields satisfactory performance in underground search [15]–[17]. Difficulties associated with diffusion dominated odor dispersal model led to the development of reactive plume tracking approaches, the performance of which was further improved by combining vision with sensing [18]–[20]. The efficiency of techniques depending heavily on sensing, such as chemotaxis [21]; anemotaxis [6], [22]; infotaxis [7]; fluxotaxis [23] and their close variants are limited by the quality of sensors and the manner in which they are used. Bio-inspired agent maneuvering such as Braitenberg style [24], *E. coli* algorithm [10], zigzag dung beetle approach [25], and silkworm moth style [15], [26], [27] are slow in localization. Many of these localizing techniques deliver unsatisfactory tracking performance in a turbulence dominated environment.

With advantages of multiagent systems such as spatial diversity, distributed sensing and actuation, redundancy, scalability, high reliability, and increased probability of success, OSL can be effectively solved. This dynamical optimization problem is characterized by three stages: 1) instantaneous plume sensing (plume finding); 2) maneuvering of the agents (plume traversal); and 3) cooperative control of the agents. In spite of growing attention from researchers in the last decade [28]–[31], only a few works have addressed OSL using MAS. A distributed cooperative algorithm based on swarm intelligence was put forth by Hayes *et al.* [32] and experimental results proved multiple robots perform more efficiently than a single autonomous robot. Marques *et al.* [33] proposed particle swarm optimization (PSO) algorithm [34] to localize odor source. Studies in [35] reported modified PSO technique based on electrical charge theory by using neutral and charged robots to find the odor source without getting trapped into a local maximum concentration. Cooperative control based on simplified PSO was proposed by Lu *et al.* [36], which is a type of proportional-only controller and the operating region is confined between the global and the local best. This requires complicated obstacle avoidance algorithms and more energy consumption. Odor propagation is nontrivial, i.e., odor arrives in packets, leading to wide fluctuations in measured concentrations. Plumes also tend to be dynamic and turbulent. In order to effectively solve OSL problem, information of wind needs

Manuscript received January 18, 2018; revised May 6, 2018; accepted September 2, 2018. This paper was recommended by Associate Editor L. Zhang. (*Corresponding author: Abhinav Sinha*.)

A. Sinha is with the Indian Institute of Technology Bombay, Mumbai, India (e-mail: sinha.abhinav@iitb.ac.in).

R. Kumar, R. Kaur, and A. P. Bhondekar are with CSIR-Central Scientific Instruments Organisation, Chandigarh, India (e-mail: riteshkr@csio.res.in; rishemjit.kaur@csio.res.in; amolbhondekar@csio.res.in).

This paper has supplementary downloadable material available at <http://ieeexplore.ieee.org>, provided by the author.

Color versions of one or more of the figures in this paper are available online at <http://ieeexplore.ieee.org>.

Digital Object Identifier 10.1109/TCYB.2018.2869224

83 to be taken into consideration. As odor molecules travel down-
 84 wind, direction of wind provides an effective information on
 85 relative position of the source. Using both concentration and
 86 wind information, Lu and Han have designed a particle filter-
 87 based cooperative control scheme [37] to coordinate multiple
 88 robots toward odor source. However, the dynamical model
 89 used in [36] and [37] are oversimplified to integrator dynamics
 90 and the effects of unknown perturbations have not been con-
 91 sidered. To address the effect of perturbations, robust control
 92 protocols have been designed in [8] and [38], but dynamics of
 93 the agents is homogeneous, i.e., agents are identical. In prac-
 94 tice, it is very difficult to obtain truly homogeneous agents.
 95 Even truly homogeneous agents exhibit a tendency to drift
 96 toward heterogeneity over time and continued operation.

97 In spite of rapid developments in sensor technology, avail-
 98 ability of faster localization algorithms are still a challenge.
 99 Motivated by these studies and in order to effectively address
 100 the OSL problem, we have proposed a three-layered hierar-
 101 chical cooperative control scheme which uses concentraion
 102 information from swarm, as well as wind information from a
 103 measurement model [39] describing movement of filaments to
 104 locate the odor source. Information about the source via instan-
 105 taneous sensing and swarm intelligence is obtained in the first
 106 layer. Second layer is designed to maneuver the agents via tra-
 107 ditional surging, casting, and searching methods. Third layer is
 108 the cooperative control layer and the controller is based on the
 109 paradigms of variable structure control [also known as sliding
 110 mode control (SMC)], which is known for its inherent robust-
 111 ness and properties to reject disturbances that lie in the range
 112 space of input. In the third layer, the information obtained in
 113 the first layer is passed as a reference to the tracking controller.
 114 A block diagram representation of the proposed scheme has
 115 been shown in Fig. 1.

116 The idea of using a finite time controller is not new, how-
 117 ever, we have adopted a different perspective in this paper.
 118 To the best of authors' knowledge, SMC technique has been
 119 used for the first time in OSL. Novel sliding manifold and
 120 reaching law provide faster convergence. The sole idea to
 121 use such a control is to guarantee faster convergence, com-
 122 plete disturbance rejection, and steady precision. Moreover,
 123 studies in this paper incorporate a large class of systems
 124 that may contain unknown inherent nonlinearity and hetero-
 125 geneity. We summarize our contributions via the following
 126 points.

- 127 1) Individual autonomous agents may have some inherent
 128 nonlinear dynamics. This paper generalizes the problem
 129 by taking into account nonlinear dynamics of MAS.
 130 When the uncertain function is zero, the dynamics
 131 simply reduces to that of an integrator system.
- 132 2) Individual autonomous agents might have different
 133 dynamics for a practical application. Hence, the con-
 134 sideration of heterogeneous agent dynamics is closer to
 135 real situations.
- 136 3) The finite time robust controller is based on sliding
 137 modes with nonlinear sliding hyperplane and novel
 138 inverse sine hyperbolic reaching law. Consequently, the
 139 control signal is smooth and reachability to the manifold
 140 is fast.

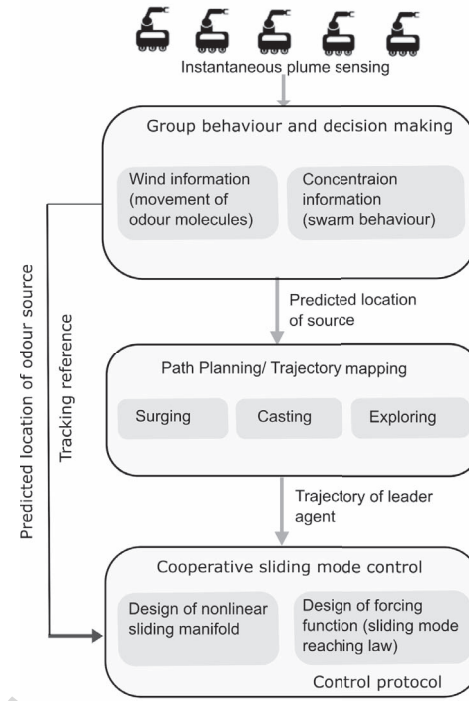


Fig. 1. Proposed hierarchical cooperative control scheme for odor source localization.

141 4) The synthesized control ensures stability even in the
 142 presence of disturbances that are bounded and matched.
 143 After introduction to the study in Section I, remainder of this
 144 paper is organized as follows. Section II provides insights into
 145 preliminaries of spectral graph theory and SMC. Section III
 146 presents dynamics of MAS and mathematical problem for-
 147 mulation, followed by hierarchical decentralized cooperative
 148 control scheme in Section IV. Results and discussions have
 149 been carried out in Section V, followed by concluding remarks
 150 in Section VI. We have provided a supplement to this paper
 151 with some additional illustrations to aid the propositions.

II. PRELIMINARIES

A. Spectral Graph Theory for Multiagent Systems

152 A directed graph, also known as digraph is represented
 153 throughout in this paper by $\mathcal{G} = (\mathcal{V}, \mathcal{E}, \mathcal{A})$. \mathcal{V} is the nonempty
 154 set in which finite number of vertices or nodes are contained
 155 such that $\mathcal{V} = \{1, 2, \dots, N\}$. \mathcal{E} denotes directed edge and is
 156 represented as $\mathcal{E} = \{(i, j) \forall i, j \in \mathcal{V} \& i \neq j\}$. \mathcal{A} is the weighted
 157 adjacency matrix such that $\mathcal{A} = a(i, j) \in \mathbb{R}^{N \times N}$. The possi-
 158 bility of existence of an edge (i, j) occurs if and only if the
 159 vertex i receives the information supplied by the vertex j , i.e.,
 160 $(i, j) \in \mathcal{E}$. Hence, i and j are termed neighbors. The set \mathcal{N}_i
 161 contains labels of vertices that are neighbors of the vertex i . For
 162 the adjacency matrix \mathcal{A} , $a(i, j) \in \mathbb{R}_0^+$. If $(i, j) \in \mathcal{E} \Rightarrow a(i, j) >$
 163 0. If $(i, j) \notin \mathcal{E}$ or $i = j \Rightarrow a(i, j) = 0$. The Laplacian matrix
 164 \mathcal{L} [40] is central to the consensus problem and is given by
 165 $\mathcal{L} = \mathcal{D} - \mathcal{A}$ where degree matrix, \mathcal{D} is a diagonal matrix, i.e.,
 166 $\mathcal{D} = \text{diag}(d_1, d_2, \dots, d_n)$ whose entries are $d_i = \sum_{j=1}^n a(i, j)$.
 167 A directed path from vertex j to vertex i defines a sequence
 168 comprising of edges $(i_1, i_1), (i_1, i_2), \dots, (i_l, j)$ with distinct ver-
 169 tices $i_k \in \mathcal{V}, k = 1, 2, 3, \dots, l$. Incidence matrix \mathcal{B} is also a
 170

diagonal matrix with entries 1 or 0. The entry is 1 if there exists an edge between leader agent and any other agent, otherwise it is 0. Furthermore, it can be inferred that the path between two distinct vertices is not uniquely determined. However, if a distinct node in \mathcal{V} contains directed path to every other distinct node in \mathcal{V} , then the directed graph \mathcal{G} is said to have a spanning tree. Consequently, the matrix $\mathcal{L} + \mathcal{B}$ has full rank [40]. Physically, each agent has been modeled by a vertex or node and the line of communication between any two agents has been modeled as a directed edge.

182 B. Sliding Mode Control

SMC [41] is known for its inherent robustness. The switching nature of the control is used to nullify bounded disturbances and matched uncertainties. Switching happens about a hypergeometric manifold in state space known as sliding manifold, surface, or hyperplane. The control drives the system monotonically toward the sliding surface, i.e., trajectories emanate and move toward the hyperplane (reaching phase). System trajectories, after reaching the hyperplane, get constrained there for all future time (sliding phase), thereby ensuring the system dynamics remains independent of bounded disturbances and matched uncertainties.

In order to push state trajectories onto the surface $s(x)$, a proper discontinuous control effort $u_{\text{SM}}(t, x)$ needs to be synthesized satisfying the inequality

$$197 \quad s^T(x)\dot{s}(x) \leq -\eta \|s(x)\| \quad (1)$$

with η being positive and is referred as the reachability constant

$$200 \quad \therefore \dot{s}(x) = \frac{\partial s}{\partial x}\dot{x} = \frac{\partial s}{\partial x}f(t, x, u_{\text{SM}}) \quad (2)$$

$$201 \quad \therefore s^T(x)\frac{\partial s}{\partial x}f(t, x, u_{\text{SM}}) \leq -\eta \|s(x)\|. \quad (3)$$

The motion of state trajectories confined on the manifold is known as *sliding*. Sliding mode exists if the state velocity vectors are directed toward the manifold in its neighborhood. Under such consideration, the manifold is called attractive, i.e., trajectories starting on it remain there for all future time and trajectories starting outside it tend to it in an asymptotic manner. Hence, in sliding motion

$$209 \quad \dot{s}(x) = \frac{\partial s}{\partial x}f(t, x, u_{\text{SM}}) = 0. \quad (4)$$

$u_{\text{SM}} = u_{\text{eq}}$ is a solution, generally referred as equivalent control, is not the actual control applied to the system but can be thought of as a control that must be applied on an average to maintain sliding motion, and is mainly used for analysis of sliding motion.

215 III. DYNAMICS OF MAS AND PROBLEM FORMULATION

Consider first-order heterogeneous MAS with a virtual leader and a finite number of followers interacting among themselves and their environment in a well-defined directed topology. Via interagent communication, only local information about the predicted location of source of the odor

through instantaneous plume sensing is available. The governing dynamics of first-order heterogeneous MAS that comprise of N agents can be written mathematically as

$$221 \quad \dot{x}_i(t) = f_i(x_i(t)) + u_{\text{SM}_i}(t) + \xi_i; i \in [1, N] \in \mathbb{N} \quad (5) \quad 224$$

where $f_i(\cdot)$ denotes the uncertain dynamics of each agent. x_i and u_{SM_i} are the state of i th agent and the associated control, respectively. ξ_i represents bounded exogenous disturbances that enter the system from input channel, i.e., $\|\xi_i\| \leq \xi_{\max} < \infty$. There is always a limit on how fast a function can change. Considering the functions describing the dynamics (5) do not become infinitely steep at some point, it is safe to assume that the functions satisfy Lipschitz continuity.

Assumption 1: $f_i(\cdot) : \mathbb{R}^+ \times X \rightarrow \mathbb{R}^m$ is locally Lipschitz over some domain $\mathbb{D}_{\mathbb{L}}$ with Lipschitz constant \bar{L} . For our case, we shall take this domain $\mathbb{D}_{\mathbb{L}}$ to be fairly large. $X \subset \mathbb{R}^m$ is a domain in which origin is contained.

Since the function $f_i(\cdot)$ is uncertain, a nominal system model can be extracted from the known part of the uncertain function $f_i(\cdot)$, and the unknown part can be treated by worst case bounds. The dynamics of each agent is affected by the interconnection among agents as well as the presence of inherent nonlinearity in each agent. Note that when $f_i(\cdot) = 0$, the dynamics reduce to those of integrator systems. Similarly, when $f_i(\cdot)$ are all same, we obtain a set of homogeneous agents.

Remark 1: For the sake of simplicity, we shall carry out the discussion in \mathbb{R}^1 . However, the same can be extended to higher dimensions by the use of Kronecker products.

Odor molecules tend to disperse heavily in the environment characterized by diffusion. In making assumptions of a diffusion dominated environment, several factors are ignored. A more realistic picture must include effects of wind, turbulence diffusion, and thermal effects. However, effects of turbulence are difficult to be described mathematically. In addition to the effects of wind, the characteristics of environment can also be described by advection phenomenon. Hence, we have considered a diffusion–advection plume model in our discussed source localization problem. Before we begin to use this model, the following assumptions need to be stated.

Assumption 2: We assume near uniform airflow velocity for all time and throughout the domain in which the task of source localization is being performed.

If the domain is characterized by nonuniform airflow velocity, the concentration of odor molecules in a particular region shall vary too rapidly with time and could possibly result in loss of effective sensing, disordering of swarm, and delayed consensus.

Assumption 3: The turbulence diffusion coefficient K needs to be known beforehand via some suitable measurements. In case K is not known beforehand, then K should be estimated or correlated as a function of wind velocity, i.e., $K = f(v_a)$. This estimation can be performed during the experiment with the data obtained through sensors (e.g., anemometers and gas sensors).

Knowledge of these parameters is essential in algorithm research. These parameters influence the overall effective sensing and accuracy of the prediction of odor source location (the global concentration maxima.) The diffusion–advection model

278 provided in [42] and [43] has been recalled here to simulate
 279 the dynamic plume under time varying disturbances. A steady
 280 concentration profile for a very large span of time ($t \rightarrow \infty$)
 281 can be written as

$$282 \quad C(\vec{r}, \infty) = \frac{q_0}{2\pi K d_i} \exp\left\{-\frac{v_a}{2K}(d_i - \vec{r} + \vec{r}_0)\right\}. \quad (6)$$

283 In (6), $\vec{r}_0 = x_s(t)$ represents the coordinates of the odor
 284 source, $d_i = \|x_i - x_s\|$, q_0 is the filament release rate and
 285 K is the turbulent diffusion coefficient that is independent of
 286 the diffusing material.

287 The problem of odor source localization can be viewed as a
 288 cooperative control problem in which control laws u_{SM_i} need
 289 to be designed such that the conditions $\lim_{t \rightarrow \infty} \|x_i - x_j\| = 0$
 290 and $\lim_{t \rightarrow \infty} \|x_i - x_s\| \leq \theta$ are satisfied. Here, x_s represents
 291 the probable location of odor source and θ is an accuracy
 292 adjustment parameter in declaration of the true location of the
 293 source.

294 IV. HIERARCHICAL DECENTRALIZED COOPERATIVE 295 CONTROL SCHEME

296 In order to force the agents in consensus to locate the source
 297 of odor, we have come up with the following hierarchical
 298 scheme.

299 A. Group Decision Making

300 This layer utilizes both concentration and wind information
 301 to predict the location of odor source. Thus, the final probable
 302 position of the source can be described as

$$303 \quad \phi(t_h) = k_1 p_i(t_h) + (1 - k_1) q_i(t_h). \quad (7)$$

304 With the knowledge of PSO, $p_i(t_h)$ in (7) can be described as
 305 the oscillation center. Information of the wind is captured in
 306 $q_i(t_h)$. $k_1 \in (0, 1)$ denotes additional weighting coefficient.

307 *Remark 2:* Since the sensors equipped with the agents can
 308 only receive data at discrete instants, the arguments in (7)
 309 represent data captured at $t = t_h$ instants ($h = 1, 2, \dots$).

310 It should be noted that ϕ is the tracking reference that is fed
 311 to the tracking controller. Now, we present detailed description
 312 of obtaining $p_i(t_h)$ and $q_i(t_h)$.

313 Commonly used simple PSO algorithm can be described in
 314 the following form:

$$315 \quad v_i(t_{h+1}) = \omega v_i(t_h) + u_{PSO}(t_h) \quad (8)$$

$$316 \quad x_i(t_{h+1}) = x_i(t_h) + v_i(t_{h+1}). \quad (9)$$

317 Here, ω is the inertia factor, $v_i(t_h)$ and $x_i(t_h)$ represent the
 318 respective velocity and position of i th agent. This commonly
 319 used form of PSO can also be used as a proportional-only type
 320 controller, however, for the disadvantages highlighted earlier,
 321 we do not regard PSO as our final controller. PSO control law,
 322 u_{PSO} can be described as

$$323 \quad u_{PSO} = \alpha_1(x_l(t_h) - x_i(t_h)) + \alpha_2(x_g(t_h) - x_i(t_h)). \quad (10)$$

324 In (10), $x_l(t_h)$ denotes the previous best position and $x_g(t_h)$
 325 denotes the global best position of neighbors of i th agent
 326 at time $t = t_h$, and α_1 and α_2 are acceleration coefficients.
 327 Since, every agent in MAS can get some information about the

328 magnitude of concentration via local communication, position
 329 of the agent with the global best can be easily known. By the
 330 idea of PSO, we can compute the oscillation center $p_i(t_h)$ as

$$331 \quad p_i(t_h) = \frac{\alpha_1 x_l(t_h) + \alpha_2 x_g(t_h)}{\alpha_1 + \alpha_2} \quad (11)$$

332 where

$$333 \quad x_l(t_h) = \arg \max_{0 < t < t_{h-1}} \{g(x_l(t_{h-1})), g(x_i(t_h))\} \quad (12)$$

$$334 \quad x_g(t_h) = \arg \max_{0 < t < t_{h-1}} \left\{ g(x_g(t_{h-1})), \max_{j \in N} a_{ij} g(x_j(t_h)) \right\}. \quad (13)$$

335 Thus, from (10) and (11)

$$336 \quad u_{PSO}(t_h) = (\alpha_1 + \alpha_2)\{p_i(t_h) - x_i(t_h)\} \quad (14)$$

337 which is clearly a proportional-only controller with propor-
 338 tional gain $\alpha_1 + \alpha_2$, as highlighted earlier.

339 In order to compute $q_i(t_h)$, movement process of a single fil-
 340 ament that consists several odor molecules has been modeled
 341 based on the study in [39]. If $x_f(t)$ denotes position of the fil-
 342 ament at time t , $\bar{v}_a(t)$ represent mean airflow velocity and $n(t)$
 343 be some random process, then the model can be described as

$$344 \quad x_f(t) = \bar{v}_a(t) + n(t). \quad (15)$$

345 Without loss of generality, we shall regard the start time of
 346 our experiment as $t = 0$. From (15), we have

$$347 \quad x_f(t) = \int_0^t \bar{v}_a(\tau) d\tau + \int_0^t n(\tau) d\tau + x_s(0). \quad (16)$$

348 $x_s(0)$ denotes the real position of the odor source at $t = 0$.

349 *Assumption 4:* We assume the presence of a single, station-
 350 ary odor source. Thus, $x_s(t) = x_s(0)$.

351 Presence of a single source implies that there is only one
 352 global concentration in the domain. Due to nontrivial nature
 353 of odor propagation, discrete packets (or puffs) containing
 354 odor molecules are obtained. Since, concentration of each puff
 355 can be measured, the global maximum concentration can be
 356 established. Implications from Remark 2 require (16) to be
 357 implemented at $t = t_h$ instants. Hence,

$$358 \quad x_f(t_h) = \sum_{m=0}^t \bar{v}_a(\tau_m) \Delta t + \sum_{m=0}^t n(\tau_m) \Delta t + x_s(t_h) \quad (17)$$

$$359 \quad x_f(t_h) = x_s(t_h) + \bar{v}_a^*(t_h) + w^*(t_h). \quad (18)$$

360 In (18), $\sum_{m=0}^t \bar{v}_a(\tau_m) \Delta t = \bar{v}_a^*(t_h)$ and $\sum_{m=0}^t n(\tau_m)$
 361 $\Delta t = w^*(t_h)$.

362 *Remark 3:* In (18), the accumulated average of $\bar{v}_a^*(t_h)$ and
 363 $w^*(t_h)$ can also be considered for all possible filament releas-
 364 ing time.

365 From (18)

$$366 \quad x_f(t_h) - \bar{v}_a^*(t_h) = x_s(t_h) + w^*(t_h). \quad (19)$$

367 The above relationship, (19) can be viewed as the information
 368 about $x_s(t_h)$ with some noise $w^*(t_h)$. Hence,

$$369 \quad q_i(t_h) = x_s(t_h) + w^*(t_h). \quad (20)$$

370 Therefore, ϕ in (7) can now be constructed from (11) and (20).
 371 To summarize, concentration information is obtained via
 372 swarm algorithm, and the wind information is obtained using
 373 a measurement model that describes the movement of odor

374 molecules. Combining this two information together gives the
 375 probable location of the odor source, which is fed to the
 376 tracking controller.

377 B. Path Planning

378 The detection of information of interest based on instant-
 379 aneous sensing of plume depends on the threshold value
 380 of sensors, and the next state is decided according to this
 381 threshold. Hence, the blueprints of trajectory planning can be
 382 described in terms of the following behavior.

- 383 1) *Surging*: If the i th agent receives data well above thresh-
 384 old, we say that some clues about the location of the
 385 source have been detected. If the predicted position of
 386 the source at $t = t_h$ as seen by i th agent be given
 387 as $x_{s_i}(t_h)$, then the next state of the agent is given
 388 mathematically as

$$389 \quad x_i(t_{h+1}) = x_{s_i}(t_h). \quad (21)$$

- 390 2) *Casting*: If the i th agent fails to detect information at any
 391 particular instant, then the next state is obtained using
 392 the following relation:

$$393 \quad x_i(t_{h+1}) = \frac{\|x_i(t_h) - x_{s_i}(t_h)\|}{2} + x_{s_i}(t_h). \quad (22)$$

- 394 3) *Search and Exploration*: If all the agents fail to detect
 395 odor clues for a time segment $[t_h, t_{h+l}] > \delta_0$ for some
 396 $l \in \mathbb{N}$ and $\delta_0 \in \mathbb{R}^+$ being the time interval for which
 397 no clues are detected or some constraint on wait time
 398 placed at the start of the experiment, then the next state
 399 is updated as

$$400 \quad x_i(t_{h+1}) = x_{s_i}(t_h) + F_\sigma^\psi. \quad (23)$$

401 In (23), F_σ^ψ is some random parameter with σ as its
 402 standard deviation and ψ as its mean.

403 C. Decentralized Control

404 In the control layer, we design a robust and powerful con-
 405 troller on the paradigms of sliding mode. It is worthy to
 406 mention that based on instantaneous sensing and swarm infor-
 407 mation, at different times, each agent can take up the role of a
 408 virtual leader whose opinion needs to be kept by other agents.
 409 The trajectory is planned by the leader agent based on surging,
 410 casting, and searching behavior. ϕ from (7) has been provided
 411 to the controller as the reference to be tracked. The tracking
 412 error is formulated as

$$413 \quad e_i(t) = x_i(t) - \phi(t_h); t \in [t_h, t_{h+1}]. \quad (24)$$

414 In terms of graph theory, we can reformulate the error
 415 variable as

$$416 \quad \epsilon_i(t) = (\mathcal{L} + \mathcal{B})e_i(t) = (\mathcal{L} + \mathcal{B})(x_i(t) - \phi(t_h)). \quad (25)$$

417 From this point onward, we shall denote $\mathcal{L} + \mathcal{B}$ as \mathcal{H} . Next,
 418 we propose the nonlinear sliding manifold

$$419 \quad s_i(t) = \lambda_1 \tanh(\lambda_2 \epsilon_i(t)) \quad (26)$$

420 which offers faster reachability to the surface. $\lambda_1 \in \mathbb{R}^+$
 421 represents the speed of convergence to the surface, and
 422 $\lambda_2 \in \mathbb{R}^+$ denotes the slope of the nonlinear sliding manifold.

These are coefficient weighting parameters that affect the
 423 system performance. In linear sliding manifolds, the mag-
 424 nitude of error is directly proportional to the magnitude of
 425 control effort needed to maintain sliding motion. In order
 426 to prevent violations of actuator constraints, the control
 427 effort is hard upper and lower bounded by some finite value,
 428 thereby making only a portion of the manifold attractive
 429 (termed as sliding regime). There is no guarantee of desired
 430 performance or stability outside the sliding regime. Moreover,
 431 if the reference state is too far from the current system state
 432 and the actuator saturates, the controller is unable to cope
 433 up, resulting in instability. Hence, it is beneficial to design
 434 nonlinear sliding manifolds that can hold the system states
 435 regardless of their location in the state space. 436

In general, traditional sliding mode controllers suffer from
 437 an undesirable effect of infinite frequency oscillations, known
 438 as chattering [41]. While electronic switching systems may
 439 exploit this phenomenon, mechanical hardware may result in
 440 wear and tear. Many a times, simulations engines used in
 441 numerical analysis and modeling, as well as sampling, switch-
 442 ing and delay caused by hardware used to realize the system
 443 also introduce chattering and result in excitation of unmodeled
 444 high frequency dynamics. This has an adverse effect on system
 445 performance like low control accuracy and different losses in
 446 circuits and system. Techniques to smoothen the control sig-
 447нал by making continuous approximation of the reaching law
 448 via sigmoid functions [44] also exist in literature, but then
 449 there is a tradeoff between performance and chattering. Other
 450 methods to eliminate chattering include use of higher order
 451 sliding mode techniques [45], [46] in which additional hard-
 452 ware is needed to differentiate the control signal. Traditional
 453 reaching laws in the literature of sliding mode [41], [47], [48]
 454 employ a control effort of fixed gain. In order to shorten the
 455 reaching time, a larger control input was designed, leading to
 456 chattering. On the contrary, we have designed the gain to be
 457 nonlinear by using an inverse sine hyperbolic function. This
 458 function is odd and monotonous. Whenever the trajectories are
 459 away from the surface, the gain is high and they are pulled
 460 toward the hyperplane quickly, and when the trajectories are
 461 near the hyperplane, the gain is reduced to avoid chattering.
 462 This variable gain in the reaching law results in a smoother
 463 control signal as opposed to a discontinuous one. Moreover,
 464 interdependence and propinquity of the unwanted chattering
 465 phenomenon with controller gain have been obviated [49] (see
 466 supplementary material, Section III, p. 3). 467

The forcing function has been proposed as

$$468 \quad \dot{s}_i(t) = -\mu \sinh^{-1}(m + w|s_i(t)|) \text{sign}(s_i(t)). \quad (27) \quad 469$$

In (27), m is a small offset such that the argument of $\sinh^{-1}(\cdot)$
 470 function remains nonzero and w is the gain of the controller.
 471 The parameter μ facilitates additional gain tuning. In gen-
 472 eral, $m \ll w$. This novel reaching law contains a nonlinear
 473 gain and provides faster convergence toward the manifold.
 474 Moreover, this reaching law is smooth and chattering free,
 475 which is highly desirable in mechatronic systems to ensure
 476 safe operation. 477

Theorem 1: Given the dynamics of MAS (5) connected in
 478 a directed topology, error candidates (24), (25) and the sliding
 479

480 manifold (26), the stabilizing control law that ensures accurate
481 reference tracking under consensus can be described as

$$482 \quad u_{SM_i}(t) = -\left\{ (\Lambda \mathcal{H})^{-1} \mu \sinh^{-1}(m + w|s_i(t)|) \text{sign}(s_i(t)) \Gamma^{-1} \right. \\ 483 \quad \left. + (f(x_i(t)) - \dot{\phi}(t_h)) \right\} \quad (28)$$

484 where $\Lambda = \lambda_1 \lambda_2$, $\Gamma = 1 - \tanh^2(\lambda_2 \epsilon_i(t))$, $w > \sup_{t \geq 0} \{\|\zeta_i\|\}$
485 & $\mu > \sup\{\|\Lambda \mathcal{H} \zeta_i \Gamma\|\}$.

486 *Remark 4:* As mentioned earlier, $\lambda_1, \lambda_2 \in \mathbb{R}^+$. This ensures
487 $\Lambda \neq 0$ and hence its nonsingularity. The argument of $\tanh(\cdot)$
488 is always finite and satisfies $\lambda_2 \epsilon_i(t) \neq \pi \iota(\kappa + 1/2)$ for $\kappa \in \mathbb{Z}$,
489 thus Γ is also invertible. Moreover, the nonsingularity of \mathcal{H}
490 can be established directly if the digraph contains a spanning
491 tree with leader agent as a root.

492 *Proof:* From (25) and (26), we can write

$$493 \quad \dot{s}_i(t) = \lambda_1 \left\{ \lambda_2 \dot{\epsilon}_i(t) \left(1 - \tanh^2(\lambda_2 \epsilon_i(t)) \right) \right\} \quad (29)$$

$$494 \quad = \lambda_1 \lambda_2 \dot{\epsilon}_i(t) - \lambda_1 \lambda_2 \dot{\epsilon}_i(t) \tanh^2(\lambda_2 \epsilon_i(t)) \quad (30)$$

$$495 \quad = \lambda_1 \lambda_2 \dot{\epsilon}_i(t) \left\{ 1 - \tanh^2(\lambda_2 \epsilon_i(t)) \right\} \quad (31)$$

$$496 \quad = \Lambda \mathcal{H} (\dot{x}_i(t) - \dot{\phi}(t_h)) \Gamma \quad (32)$$

497 with Λ and Γ as defined in Theorem 1. From (5), (32) can be
498 further simplified as

$$499 \quad \dot{s}_i(t) = \Lambda \mathcal{H} (f(x_i(t)) + u_{SM_i}(t) + \zeta_i - \dot{\phi}(t_h)) \Gamma. \quad (33)$$

500 Using (27), the control that brings the state trajectories on to
501 the sliding manifold can now be written as

$$502 \quad u_{SM_i}(t) = -\left\{ (\Lambda \mathcal{H})^{-1} \mu \sinh^{-1}(m + w|s_i(t)|) \text{sign}(s_i(t)) \Gamma^{-1} \right. \\ 503 \quad \left. + (f(x_i(t)) - \dot{\phi}(t_h)) \right\}$$

504 which is same as (28), thereby completing the proof. ■

505 *Remark 5:* The control (28) can be practically implemented
506 as it does not contain the uncertainty term.

507 It is crucial to analyze the necessary and sufficient conditions
508 for the existence of sliding mode when control protocol
509 col (28) is used. We regard the system to be in sliding mode
510 if for any time $t_1 \in [0, \infty)$, system trajectories are brought
511 upon the manifold $s_i(t) = 0$ and are constrained there for all
512 time thereafter, i.e., for $t \geq t_1$, sliding motion occurs.

513 *Theorem 2:* Consider the system described by (5), error
514 candidates (24), (25), sliding manifold (26), and the control
515 protocol (28). Sliding mode is said to exist in vicinity of sliding
516 manifold, if the manifold is attractive, i.e., trajectories
517 emanating outside it continuously decrease toward it. Stating
518 alternatively, reachability to the surface is ensured for some
519 reachability constant $\eta > 0$. Further, stability can be guaranteed
520 in the sense of Lyapunov if gain μ is designed as
521 $\mu > \sup\{\|\Lambda \mathcal{H} \zeta_i \Gamma\|\}$.

522 *Proof:* Let us take into account, a Lyapunov function
523 candidate

$$524 \quad V_i = 0.5 s_i^2. \quad (34)$$

525 Taking derivative of (34) along system trajectories yield

$$526 \quad \dot{V}_i = s_i \dot{s}_i \quad (35)$$

$$527 \quad = s_i \{ \Lambda \mathcal{H} (f(x_i(t)) + u_{SM_i}(t) + \zeta_i - \dot{\phi}(t_h)) \Gamma \}. \quad (36)$$

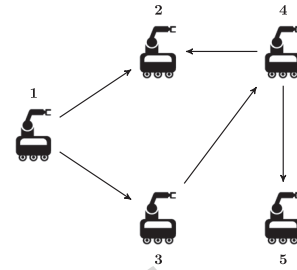


Fig. 2. Topology in which agents are connected.

Substituting the control protocol (28) in (36), we have

$$\begin{aligned} \dot{V}_i &= s_i \left(-\mu \sinh^{-1}(m + w|s_i|) \text{sign}(s_i) + \Lambda \mathcal{H} \zeta_i \Gamma \right) \\ &= -\mu \sinh^{-1}(m + w|s_i|) \|s_i\| + \Lambda \mathcal{H} \zeta_i \Gamma \|s_i\| \\ &= \left\{ -\mu \sinh^{-1}(m + w|s_i|) + \Lambda \mathcal{H} \zeta_i \Gamma \right\} \|s_i\| \\ &= -\eta \|s_i\| \end{aligned} \quad (37)$$

where $\eta = \mu \sinh^{-1}(m + w|s_i|) - \Lambda \mathcal{H} \zeta_i \Gamma > 0$ is called
reachability constant. For $\mu > \sup\{\|\Lambda \mathcal{H} \zeta_i \Gamma\|\}$, we have

$$\dot{V}_i < 0. \quad (38)$$

Thus, the derivative of Lyapunov function candidate is negative
definite confirming stability in the sense of Lyapunov.

Since, $\mu > 0$, $\|s_i\| > 0$ and $\sinh^{-1}(\cdot) > 0$ due to the nature
of its arguments. Therefore, (27) and (37) together provide
implications that $\forall s_i(0)$, $s_i \dot{s}_i < 0$ and the surface is globally
attractive. This completes the proof. ■

V. RESULTS AND DISCUSSIONS

Fig. 2 depicts the interaction topology of the agents [8] as
a digraph. In theory, the control has been synthesized using
 \mathcal{H} matrix. If the elements of \mathcal{H} are constant, the topology is
fixed, and if the elements of \mathcal{H} are time-varying, the connection
represents a switching topology. Note that although the
developed theory and hierarchical scheme can be extended to
a switching topology as well, we shall simplify the case by
taking a fixed topology.

Assumption 5: Agent 1 appears as the virtual leader to all
other agents. Therefore, the topology is fixed and directed.

The associated graph matrices have been described as

$$\mathcal{A} = \begin{bmatrix} 0 & 0 & 1 & 0 \\ 0 & 0 & 0 & 0 \\ 0 & 1 & 0 & 0 \\ 0 & 0 & 1 & 0 \end{bmatrix}, \quad \mathcal{B} = \begin{bmatrix} 1 & 0 & 0 & 0 \\ 0 & 1 & 0 & 0 \\ 0 & 0 & 0 & 0 \\ 0 & 0 & 0 & 0 \end{bmatrix} \quad (554)$$

$$\mathcal{D} = \begin{bmatrix} 1 & 0 & 0 & 0 \\ 0 & 0 & 0 & 0 \\ 0 & 0 & 1 & 0 \\ 0 & 0 & 0 & 1 \end{bmatrix} \quad (555)$$

$$\mathcal{L} = \mathcal{D} - \mathcal{A} = \begin{bmatrix} 1 & 0 & -1 & 0 \\ 0 & 0 & 0 & 0 \\ 0 & -1 & 1 & 0 \\ 0 & 0 & -1 & 1 \end{bmatrix} \quad (556)$$

$$\mathcal{L} + \mathcal{B} = \begin{bmatrix} 2 & 0 & -1 & 0 \\ 0 & 1 & 0 & 0 \\ 0 & -1 & 1 & 0 \\ 0 & 0 & -1 & 1 \end{bmatrix}. \quad (39) \quad (557)$$

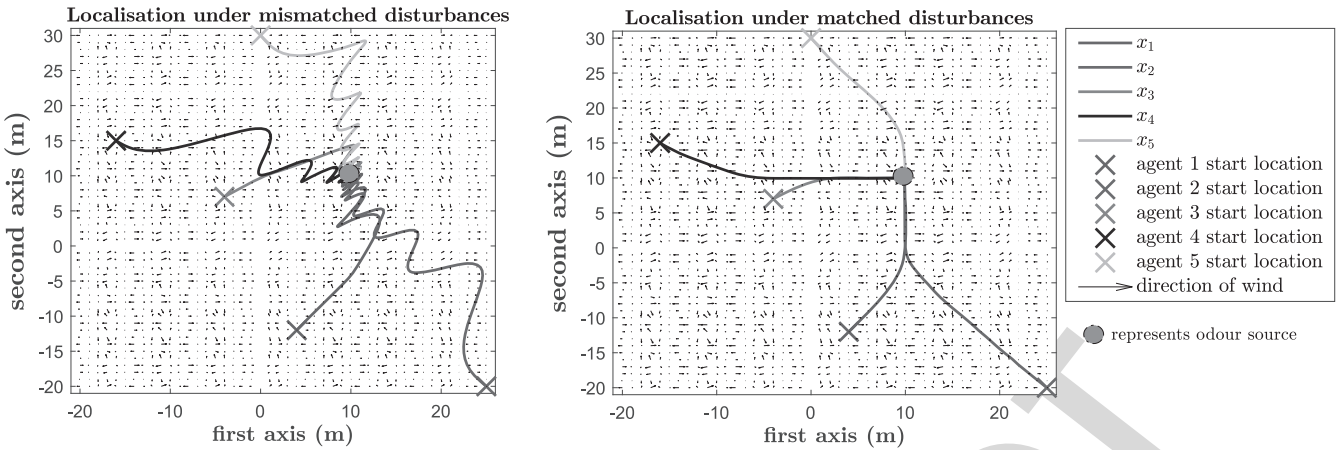


Fig. 3. Localization by MAS under the effect of mismatched and matched disturbances.

TABLE I
VALUES OF THE DESIGN PARAMETERS USED IN SIMULATION

k_1	ω_{max}	α_1	α_2	λ_1	λ_2	μ	m	w
0.5	2 rad/s	0.25	0.25	1.774	2.85	5	10^{-3}	2

TABLE II
FOUR CASES OF LOCALIZATION CONSIDERED IN THIS PAPER

Technique	Consensus	Formation	Matched perturbations	Mismatched perturbations
Case 1	✓	✗	✓	✗
Case 2	✗	✓	✓	✗
Case 3	✓	✗	✗	✓
Case 4	✗	✓	✗	✓

558 Dynamics of the agents are described as

$$\dot{x}_1 = 0.1\sqrt{3}\sin(x_1) + \cos(2\pi t) + u_{SM_1}(t) + \varsigma_1 \quad (40)$$

$$\dot{x}_2 = 0.1\sin(x_2) - \cos(e^{-x_2 t}) + u_{SM_2}(t) + \varsigma_2 \quad (41)$$

$$\dot{x}_3 = 0.1\sqrt{3}\sin(x_3) + \cos^2(2\pi t) + u_{SM_3}(t) + \varsigma_3 \quad (42)$$

$$\dot{x}_4 = 0.1\sin(x_4) + \cos(x_4) + u_{SM_4}(t) + \varsigma_4 \quad (43)$$

$$\dot{x}_5 = 0.1\cos(x_5) - \cos(2\pi t) - e^{-t} + u_{SM_5}(t) + \varsigma_5. \quad (44)$$

564 Initial conditions have been chosen to be far from the equi-
565 librium point. We shall consider a time varying disturbance
566 $\varsigma_i = 0.3\sin(\pi^2 t^2)$ for matched case and $\varsigma_i = 20\sin(\pi^2 t^2)$
567 for mismatched (or, unmatched) case, accuracy parameter
568 $\theta = 0.001$ and maximum mean airflow velocity $\bar{v}_{a_{max}} = 1$ m/s.
569 Other key design parameters are provided in Table I.

570 Turbulence coefficient, K , is taken to be $0.02 \text{ m}^2/\text{s}$ and fila-
571 ment release rate, $q_0 = 2 \text{ mg/s}$ of diffusing substance. We
572 shall present the results for both the cases of localization
573 in \mathbb{R}^1 and \mathbb{R}^2 to demonstrate the efficiency of the designed
574 control scheme.

575 For the case of \mathbb{R}^1 , the odor source is randomly placed
576 between 10 and 11 m (see supplementary material, Section II
577 for illustrations). Agents start from various initial conditions
578 that are far from the origin and progress toward the source
579 via instantaneous plume sensing (by sensing odor molecules,
580 or filaments). As soon as the leader agent senses the odor

581 molecules, the information of predicted next state is exchanged
582 among other agents. This local information is then used to
583 make a consensus while localization. Agents come to con-
584 sensus in finite time to locate the odor source. In spite of
585 time varying disturbance, the plume tracking is accurate and
586 the localization is successful. Filaments or odor molecules
587 (source information) are released from the odor source and are
588 detected by the sensors equipped with the agents. The tracking
589 controller attempts to minimize the error between the predicted
590 next state and the actual next state. The tracking error lies in
591 the close vicinity of zero as expected, implying that the track-
592 ing error has almost been nullified. Norm of tracking errors
593 in \mathbb{R}^1 has been depicted in Fig. 4 to depict near nullification
594 of error. Novel sliding manifolds, designed in this paper, also
595 come to consensus in very short span of time, as evident from
596 Fig. 5. It is, then, quite clear that the convergence of state
597 trajectories to the sliding manifold is very fast and is highly
598 desired to ensure a high degree of robustness and autonomy.
599 Such manifolds can also be utilized to attain a desired con-
600 vergence speed by simple tuning of design parameters. Use
601 of a novel inverse sine hyperbolic reaching law results in a
602 smooth control signals for all the agents. The use of smooth
603 sliding mode controller ensures safe operation in mechatronic
604 devices. Fig. 6 depicts the control signals of all the agents
605 when localization is carried in \mathbb{R}^1 . It is clear that the signal is
606 chattering free, smooth, and accurate.

Having discussed the case of \mathbb{R}^1 , we shall now discuss
607 localization in \mathbb{R}^2 . To avoid confusion between state vari-
608 able x and axis labeled as x in the usual sense, we have
609 adopted to refer abscissa as first axis and ordinate as second
610 axis throughout this discussion. Agents are driven into consen-
611 sus to locate the odor source in \mathbb{R}^2 in the domain described
612 by the axis limits. Within the domain of localization, a total
613 of 25 trials were done with various initial conditions cho-
614 sen far from the origin. Fig. 7 shows the average time spent
615 in four cases—localization via consensus under matched per-
616 turbations (case 1), localization via formation under matched
617 perturbations (case 2), localization via consensus under mis-
618 matched perturbations (case 3), and localization via formation
619 under mismatched perturbations (case 4). Similar to the results
620 in [50], the success rate of this technique is also 100% except
621

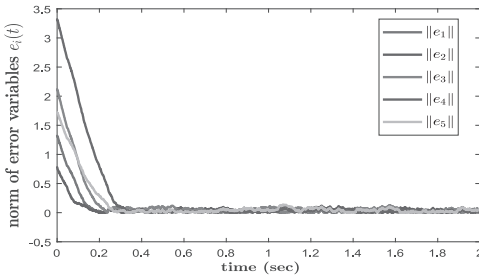
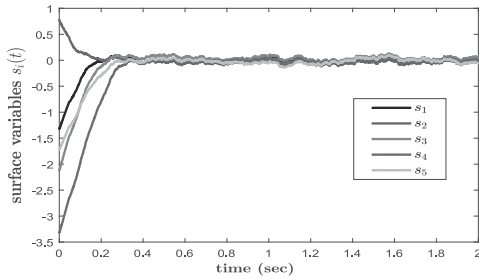
Fig. 4. Localization tracking errors in \mathbb{R}^1 .

Fig. 5. Sliding manifolds during consensus.

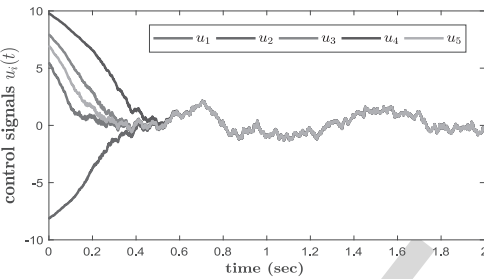


Fig. 6. Smooth control signals of all the agents during consensus.

for the fact that time spent in localization is lesser via this technique owing to faster convergence of state trajectories to the sliding manifold. The four cases have been illustrated here in a tabular format for ease of reference. A check (cross) mark in a particular column indicates that the particular strategy has been used (not used) in localization.

We shall also present two cases under which localization has been tasked: 1) under consensus and 2) under parallel formation. Note that agents may be subjected to any geometrical pattern, or formation that deems suitable for the task at hand. In Figs. 8 and 9, norms of tracking errors along first and second axis have been depicted. Similar to the error profile in Fig. 4, the tracking is accurate and the agents are able to complete the localization task in finite time. For a random trial, Fig. 3 shows localization in a turbulent environment under the effect of both mismatched and matched disturbances. Under mismatched disturbances and turbulence, localization takes slightly more time as compared with its matched disturbance counterpart. The domain for this task has been set to be a grid of 50×50 along both the axes. Abscissa ranges from -20 to 30 , and so does the ordinate. Start position of agents are denoted by a “ \times ” in five different colors. Filaments or the odor molecules are released from the odor source and

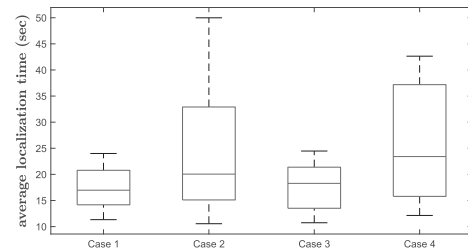


Fig. 7. Average localization time for 25 trials.

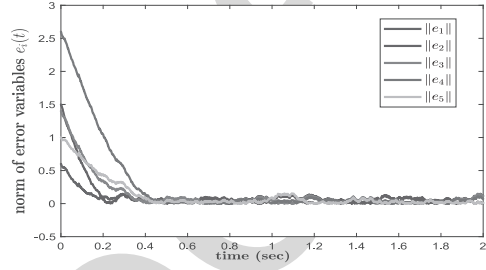


Fig. 8. Localization tracking errors along first axis.

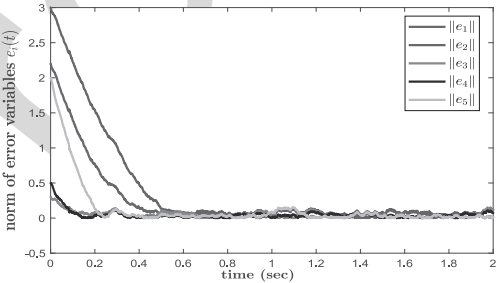


Fig. 9. Localization tracking errors along second axis.

TABLE III
PERFORMANCE METRICS IN CONTEXT OF LOCALIZATION

Technique	Average Success rate	Median localisation Time	Control Implementation
Case 1 (this study)	100%	16 sec	Time-triggered
Case 2 (this study)	100%	20 sec	Time-triggered
Case 3 (this study)	100%	18 sec	Time-triggered
Case 4 (this study)	100%	22 sec	Time-triggered
PSO [33]	21.5%	986.25 sec	Time-triggered
FTMCS [50]	100%	137.5 sec	Time-triggered

the molecules disperse in the domain characterized by heavy turbulence. Performance metrics of localization in terms of average time spent in locating the source of odor have been provided in Table III. For best case scenario of localization in \mathbb{R}^2 , please refer the supplementary material, Section II.

Finally, we state some limitations of the current approach. If the domain of localization is very large, the number of agents should increase in order to effectively solve OSL problem. However, increase in number of agents shall add to the economy, and there is a cost to maintain the communication links. Further, anomalies such as packet dropout, link failure, and latencies in communication should be carefully checked. Another scenario where localization is quite difficult, if not impossible, is the presence of multiple time varying global maxima and local minima. This shall render MAS slightly confused and a different approach should be adopted, such as

extrapolating the location based on known (or probable) presence of the source. All these issues shall be addressed in our future studies sequentially.

VI. CONCLUSION

In this paper, odor source localization via multiagent systems has been addressed. The localizing task is based on a cooperative strategy where agents interact locally among themselves to locate the source of odor in finite time. A hierarchical control scheme has been developed to predict the probable location of odor source using information of wind and concentration. This control scheme based on PSO and SMC is robust and insensitive to matched disturbances. Numerical simulations demonstrate the effectuality of the proposed scheme for both cases 1) when agents localize the odor source via consensus and 2) parallel formation. The localization takes very less time compared to other strategies and the success rate is 100%. In future, we shall address the communication issues associated with the problem.

COMPETING INTERESTS

The authors declare that there are no competing interests associated with this paper.

REFERENCES

- [1] G. S. Settles, "Sniffers: Fluid-dynamic sampling for olfactory trace detection in nature and homeland security—The 2004 freeman scholar lecture," *J. Fluids Eng.*, vol. 127, no. 2, pp. 189–218, Feb. 2005, doi: 10.1115/1.1891146.
- [2] D. W. Gage, "Many-robot MCM search systems," in *Proc. Auton. Veh. Mine Countermeas. Symp.*, 1995, pp. 9–55.
- [3] H. Ishida, T. Nakamoto, T. Moriizumi, T. Kikas, and J. Janata, "Plume-tracking robots: A new application of chemical sensors," *Biol. Bull.*, vol. 200, no. 2, pp. 222–226, 2001. [Online]. Available: <https://doi.org/10.2307/1543320>
- [4] V. Formisano, S. Atreya, T. Encrenaz, N. Ignatiev, and M. Giuranna, "Detection of methane in the atmosphere of Mars," *Science*, vol. 306, no. 5702, pp. 1758–1761, 2004. [Online]. Available: <http://science.sciencemag.org/content/306/5702/1758>
- [5] V. A. Krasnopolsky, J. P. Maillard, and T. C. Owen, "Detection of methane in the martian atmosphere: Evidence for life?" *Icarus*, vol. 172, no. 2, pp. 537–547, 2004. [Online]. Available: <http://www.sciencedirect.com/science/article/pii/S0019103504002222>
- [6] J. A. Farrell, S. Pang, and W. Li, "Plume mapping via hidden Markov methods," *IEEE Trans. Syst., Man, Cybern. B, Cybern.*, vol. 33, no. 6, pp. 850–863, Dec. 2003.
- [7] M. Vergassola, E. Villermoux, and B. Shraiman, "'Infotaxis' as a strategy for searching without gradients," *Nature*, vol. 445, no. 7126, pp. 406–409, 2007. [Online]. Available: <https://hal.archives-ouvertes.fr/hal-00326807>
- [8] A. Sinha, R. Kaur, R. Kumar, and A. P. Bhondekar, "Cooperative control of multi-agent systems to locate source of an odor," *ArXiv e-prints*, Nov. 2017.
- [9] X. Cui, C. T. Hardin, R. K. Ragade, and A. S. Elmaghriby, "A swarm approach for emission sources localization," in *Proc. 16th IEEE Int. Conf. Tools Artif. Intell.*, Nov. 2004, pp. 424–430.
- [10] C. Lytridis, G. S. Virk, Y. Rebour, and E. E. Kadar, "Odor-based navigational strategies for mobile agents," *Adapt. Behav.*, vol. 9, nos. 3–4, pp. 171–187, Apr. 2001, doi: 10.1177/10597123010093004.
- [11] R. Rozas, J. Morales, and D. Vega, "Artificial smell detection for robotic navigation," in *Proc. 5th Int. Conf. Adv. Robot. Unstruct. Environ. (ICAR)*, vol. 2, Jun. 1991, pp. 1730–1733.
- [12] V. Genovese, P. Dario, R. Magni, and L. Odetti, "Self organizing behavior and swarm intelligence in a pack of mobile miniature robots in search of pollutants," in *Proc. IEEE/RSJ Int. Conf. Intell. Robots Syst.*, vol. 3, Jul. 1992, pp. 1575–1582.
- [13] L. Buscemi, M. Prati, and G. Sandini, "Cellular robotics: Behaviour in polluted environments," in *Proc. 2nd Int. Symp. Distrib. Auton. Robot. Syst.*, 1994.
- [14] M. H. E. Larcombe, *Robotics in Nuclear Engineering: Computer Assisted Teleoperation in Hazardous Environments With Particular Reference to Radiation Fields*, Graham and Trotman, Inc., 1984.
- [15] R. Russell, "Chemical source location and the RoboMole project," in *Proc. Aust. Robot. Autom. Assoc.*, 2003, pp. 1–6.
- [16] R. A. Russell, "Locating underground chemical sources by tracking chemical gradients in 3 dimensions," in *Proc. IEEE/RSJ Int. Conf. Intell. Robots Syst. (IROS)*, vol. 1, Sep. 2004, pp. 325–330.
- [17] R. A. Russell, "Robotic location of underground chemical sources," *Robotica*, vol. 22, no. 1, pp. 109–115, 2004.
- [18] D. Martinez, L. Perrinet, and D. Walther, "Cooperation between vision and olfaction in a koala robot," in *Proc. Workshop Rep. Neuromorphic Eng.*, 2002, pp. 51–53.
- [19] A. Loutfi, S. Coradeschi, L. Karlsson, and M. Broxvall, "Putting olfaction into action: Using an electronic nose on a multi-sensing mobile robot," in *Proc. IEEE/RSJ Int. Conf. Intell. Robots Syst. (IROS)*, vol. 1, Sep. 2004, pp. 337–342.
- [20] H. Ishida, K. Yoshikawa, and T. Moriizumi, "Three-dimensional gas-plume tracking using gas sensors and ultrasonic anemometer," in *Proc. IEEE Sensors*, vol. 3, Oct. 2004, pp. 1175–1178.
- [21] R. A. Russell, A. Bab-Hadiashar, R. L. Shepherd, and G. G. Wallace, "A comparison of reactive robot chemotaxis algorithms," *Robot. Auton. Syst.*, vol. 45, no. 2, pp. 83–97, 2003. [Online]. Available: <http://www.sciencedirect.com/science/article/pii/S0921889003001209>
- [22] S. Pang and J. A. Farrell, "Chemical plume source localization," *IEEE Trans. Syst., Man, Cybern. B, Cybern.*, vol. 36, no. 5, pp. 1068–1080, Oct. 2006.
- [23] D. Zarzhitsky, "Physics-based approach to chemical source localization using mobile robotic swarms," Ph.D. dissertation, Dept. Comput. Sci., Univ. Wyoming, Laramie, WY, USA, 2008.
- [24] V. Braithwaite, *Vehicles: Experiments in Synthetic Psychology*. Boston, MA, USA: MIT Press, 1984.
- [25] H. Ishida, K. Suetsugu, T. Nakamoto, and T. Moriizumi, "Study of autonomous mobile sensing system for localization of odor source using gas sensors and anemometric sensors," *Sensors Actuators A Phys.*, vol. 45, no. 2, pp. 153–157, 1994. [Online]. Available: <http://www.sciencedirect.com/science/article/pii/0924424794008299>
- [26] L. Marques and A. T. D. Almeida, "Electronic nose-based odour source localization," in *Proc. 6th Int. Workshop Adv. Motion Control*, Apr. 2000, pp. 36–40.
- [27] L. Marques, U. Nunes, and A. T. de Almeida, "Olfaction-based mobile robot navigation," *Thin Solid Films*, vol. 418, no. 1, pp. 51–58, 2002. [Online]. Available: <http://www.sciencedirect.com/science/article/pii/S004060900200593X>
- [28] C. W. Reynolds, "Flocks, herds and schools: A distributed behavioral model," *SIGGRAPH Comput. Graph.*, vol. 21, no. 4, pp. 25–34, Aug. 1987. [Online]. Available: <http://doi.acm.org/10.1145/37402.37406>
- [29] W. Ren and R. W. Beard, "Consensus seeking in multiagent systems under dynamically changing interaction topologies," *IEEE Trans. Autom. Control*, vol. 50, no. 5, pp. 655–661, May 2005.
- [30] R. Olfati-Saber, J. A. Fax, and R. M. Murray, "Consensus and cooperation in networked multi-agent systems," *Proc. IEEE*, vol. 95, no. 1, pp. 215–233, Jan. 2007.
- [31] W. Yu, G. Chen, W. Ren, J. Kurths, and W. X. Zheng, "Distributed higher order consensus protocols in multiagent dynamical systems," *IEEE Trans. Circuits Syst. I, Reg. Papers*, vol. 58, no. 8, pp. 1924–1932, Aug. 2011.
- [32] A. T. Hayes, A. Martinoli, and R. M. Goodman, "Swarm robotic odor localization: Off-line optimization and validation with real robots," *Robotica*, vol. 21, no. 4, pp. 427–441, Aug. 2003, doi: 10.1017/S0263574703004946.
- [33] L. Marques, U. Nunes, and A. T. de Almeida, "Particle swarm-based olfactory guided search," *Auton. Robots*, vol. 20, no. 3, pp. 277–287, Jun. 2006. [Online]. Available: <https://doi.org/10.1007/s10514-006-7567-0>
- [34] J. Kennedy and R. Eberhart, "Particle swarm optimization," in *Proc. IEEE Int. Conf. Neural Netw.*, vol. 4, Nov. 1995, pp. 1942–1948.
- [35] W. Jatmiko, K. Sekiyama, and T. Fukuda, "A PSO-based mobile robot for odor source localization in dynamic advection-diffusion with obstacles environment: Theory, simulation and measurement," *IEEE Comput. Intell. Mag.*, vol. 2, no. 2, pp. 37–51, May 2007.
- [36] Q. Lu, S.-R. Liu, and X.-N. Qiu, "A distributed architecture with two layers for odor source localization in multi-robot systems," in *Proc. IEEE Congr. Evol. Comput.*, Jul. 2010, pp. 1–7.

- AQ8
- 801 [37] Q. Lu and Q.-L. Han, "Decision-making in a multi-robot system for odor
802 source localization," in *Proc. 37th Annu. Conf. IEEE Ind. Electron. Soc.*
803 (*IECON*), Nov. 2011, pp. 74–79.
804 [38] Q. Lu, S. Liu, X. Xie, and J. Wang, "Decision making and finite-time
805 motion control for a group of robots," *IEEE Trans. Cybern.*, vol. 43,
806 no. 2, pp. 738–750, Apr. 2013.
807 [39] J. A. Farrell, J. Murlis, X. Long, W. Li, and R. T. Cardé,
808 "Filament-based atmospheric dispersion model to achieve short
809 time-scale structure of odor plumes," *Environ. Fluid Mech.*,
810 vol. 2, no. 1, pp. 143–169, Jun. 2002. [Online]. Available:
811 <https://doi.org/10.1023/A:1016283702837>
812 [40] F. R. K. Chung, "Spectral graph theory," in *Proc. CBMS Reg. Conf. Math.*,
813 vol. 92, 1997. [Online]. Available: <http://bookstore.ams.org/cbms-92>
814 [41] K. D. Young, V. I. Utkin, and U. Ozguner, "A control engineer's guide
815 to sliding mode control," *IEEE Trans. Control Syst. Technol.*, vol. 7,
816 no. 3, pp. 328–342, May 1999.
817 [42] M. L. Cao, Q. H. Meng, Y. X. Wu, M. Zeng, and W. Li, "Consensus
818 based distributed concentration-weighted summation algorithm for gas-
819 leakage source localization using a wireless sensor network," in
820 *Proc. 32nd Chin. Control Conf.*, Jul. 2013, pp. 7398–7403.
821 [43] J. Matthes, L. Groll, and H. B. Keller, "Source localization by spatially
822 distributed electronic noses for advection and diffusion," *IEEE Trans. Signal Process.*,
823 vol. 53, no. 5, pp. 1711–1719, May 2005.
824 [44] A. Sinha and R. K. Mishra, "Nonlinear autonomous altitude control
825 of a miniature helicopter UAV based on sliding mode methodology,"
826 *Int. J. Electron. Commun. Technol.*, vol. 6, no. 1, pp. 32–37,
827 Mar. 2015. [Online]. Available: <http://www.iject.org/C2E2-2015/7-Abhinav-Sinha.pdf>
828 [45] A. Msaddek, A. Gaaloul, and F. M'sahli, *Output Feedback Robust
829 Exponential Higher Order Sliding Mode Control*. Singapore: Springer,
830 2017, pp. 53–72.
831 [46] F. Plestan, V. Brégeault, A. Glumineau, Y. Shtessel, and E. Moulay,
832 *Advances in High Order and Adaptive Sliding Mode Control—Theory
833 and Applications*. Heidelberg, Germany: Springer, 2012, pp. 465–492.
834 [47] A. Sinha and R. K. Mishra, "Control of a nonlinear continuous
835 stirred tank reactor via event triggered sliding modes," *Chem. Eng. Sci.*,
836 vol. 187, pp. 52–59, Sep. 2018. [Online]. Available:
837 <http://www.sciencedirect.com/science/article/pii/S0009250918302719>
838 [48] C. Edwards and S. K. Spurgeon, *Sliding Mode Control: Theory and
839 Applications*. London, U.K.: CRC Press, 1998.
840 [49] T. Majumder, R. K. Mishra, A. Sinha, S. S. Singh, and
841 P. K. Sahu, "Congestion control in cognitive radio networks with
842 event-triggered sliding mode," *AEU Int. J. Electron. Commun.*,
843 vol. 90, pp. 155–162, Jun. 2018. [Online]. Available:
844 <https://www.sciencedirect.com/science/article/pii/S1434841117325438>
845 [50] Q. Lu, Q. L. Han, X. Xie, and S. Liu, "A finite-time motion control strategy
846 for odor source localization," *IEEE Trans. Ind. Electron.*, vol. 61,
847 no. 10, pp. 5419–5430, Oct. 2014.
848



850 **Abhinav Sinha** received the B.Tech. degree in
851 electronics and instrumentation engineering from
852 the Kalinga Institute of Industrial Technology,
853 Bhubaneswar, India, in 2014 and the M.Tech.
854 degree in mechatronics from the Indian Institute of
855 Engineering Science and Technology, Shibpur, India,
856 in 2018.

857 He is currently a Doctoral Researcher with
858 the Dynamics and Control Group, Department
859 of Aerospace Engineering, Indian Institute of
860 Technology Bombay, Mumbai, India. He was an
861 Assistant System Engineer with the Engineering and Industrial Services
862 Division, Tata Consultancy Services (TCS) Ltd., Mumbai, from 2014 to 2016,
863 where he researched on control system integration, manufacturing execu-
864 tion systems, enterprise manufacturing intelligence, network segmentation,
865 data integration, and data security at plant level. He was also a Visiting
866 Faculty with TCS Global Learning Centre, India, in 2015. From 2017 to
867 2018, he was a Graduate Researcher with CSIR-Central Scientific Instruments
868 Organisation, Chandigarh, India, where he researched for his master's degree.
869 His current research interests include sliding mode control, event-based con-
870 trol, multiagent systems, cooperative control, and cyber-physical systems.

871 Mr. Sinha was a recipient of the IEEE Best Paper Award (IEEE Pune
872 Section & IEEE Computer Society) in 2015, On the Spot Award (TCS) in
873 2015, and the Champions of Initial Learning Programme (TCS) in 2015.
874 He is a member of the International Federation of Automatic Control,
875 Automatic Control and Dynamical Optimization Society, and the Asian
876 Control Association. He currently serves as a Reviewer for *Nonlinear
877 Dynamics* (Springer) and *IET Generation, Transmission and Distribution*.



878 **Ritesh Kumar** received the B.E. degree in com-
879 puter science and engineering from the Manipal
880 Institute of Technology, Manipal, India, in 2009 and
881 the M.Tech. degree in advanced instrumentation and
882 the Ph.D. degree from the Academy of Scientific &
883 Innovative Research, New Delhi, India, in 2011 and
884 2017, respectively.

885 Since 2011, he has been a Scientist with CSIR-
886 Central Scientific Instruments Organisation (CSIR-
887 CSIO), Chandigarh, India, working on a number of
888 government and industry-sponsored projects involv-
889 ing various domains of information and communication technology. At
890 CSIR-CSIO, he is also responsible for supervising laboratory and tutorials on
891 machine learning. He has authored and co-authored multiple journal papers.
892 His current research interests include big data analytics, perception modeling,
893 and artificial intelligence.

894 Mr. Kumar is a member of Digital Olfaction Society and the Institution of
895 Electronics and Telecommunication Engineers.



896 **Rishemjit Kaur** received the B.E. degree in elec-
897 tronics (instrumentation and control) from Thapar
898 University, Patiala, India, in 2009 and the M.Tech.
899 degree in advanced instrumentation and the Ph.D.
900 degree from the Academy of Scientific & Innovative
901 Research, New Delhi, India, in 2011 and 2017,
902 respectively.

903 She was a Research Scholar with Nagoya
904 University, Nagoya, Japan, from 2014 to 2016. Since
905 2011, she has been a Scientist with CSIR-Central
906 Scientific Instruments Organisation, Chandigarh,
907 India. She received Japanese Government scholarship for research students
908 (MEXT) from 2014 to 2016. Her current research interests include evolution-
909 ary optimization techniques, big data analytics, social network analysis, and
910 machine learning.

911 Dr. Kaur was a recipient of the Genetic and Evolutionary Computation
912 Conference Virtual Creatures Award for her research on developing controller
913 for soft-bodied robots.



914 **Amol P. Bhondekar** received the Ph.D. degree
915 in engineering from Panjab University, Chandigarh,
916 India.

917 He is with CSIR-Central Scientific Instruments
918 Organisation, Chandigarh, where he is a Principal
919 Scientist and the Head of the Department of
920 Agrionics (Post Harvest Technologies). He is also an
921 Associate Professor with the Academy of Scientific
922 and Innovative Research, New Delhi, India. He has
923 number of research articles in reputed journals to his
924 credit. His current research interests include sensors,
925 development of techniques for artificial organoleptics.

926 Dr. Bhondekar is a fellow of the Institution of Electronics and
927 Telecommunication Engineers.

AUTHOR QUERIES

AUTHOR PLEASE ANSWER ALL QUERIES

PLEASE NOTE: We cannot accept new source files as corrections for your paper. If possible, please annotate the PDF proof we have sent you with your corrections and upload it via the Author Gateway. Alternatively, you may send us your corrections in list format. You may also upload revised graphics via the Author Gateway.

AQ1: Author: Please confirm or add details for any funding or financial support for the research of this article.

AQ2: Please provide the department name and postal code for “Indian Institute of Technology Bombay, Mumbai, India” and “CSIR–Central Scientific Instruments Organisation, Chandigarh, India.”

AQ3: Please cite “Table II” inside the text.

AQ4: Figs. 4 and 9 are cited before Fig. 3. Please check if Fig. 3 can be cited earlier, or if Figs. 3–9 can be renumbered so that they are cited in sequential order.

AQ5: Please provide the complete details and exact format for Reference [8].

AQ6: Please provide the page range for References [13] and [40].

AQ7: Please provide the publisher location for Reference [14].

AQ8: Please confirm if the location and publisher information for Reference [45] and [46] is correct as set.